UNIVERSITÀ DI PARMA
ARCHIVIO DELLA RICERCA

University of Parma Research Repository

Contrasting thermophilization among forests, grasslands and alpine summits

This is the peer reviewd version of the followng article:

Original
Contrasting thermophilization among forests, grasslands and alpine summits / Yue, K., Vangansbeke, P., Myers-Smith, I.H., Waller, D.M., Verheyen, K., Bernhardt-Römermann, M., Baeten, L., Staude, I.R., Bjorkman, A.D., Hédl, R., Andrews, C., Barni, E., Becker, T., Becker-Scarpitta, A., Benito-Alonso, J.L., Bennie, J., Berki, I., Blüml, V., Brunet, J., Bullock, J.M., et al.. - In: NATURE. - ISSN 0028-0836. - (2026). [10.1038/s41586-025-09622-7]

Availability:
This version is available at: 11381/3053573 since: 2026-04-14T11:52:12Z

Publisher:
NATURE PORTFOLIO

Published
DOI:10.1038/s41586-025-09622-7

Terms of use:

Anyone can freely access the full text of works made available as "Open Access". Works made available

Publisher copyright

note finali coverpage

(Article begins on next page)

02 November 2026

Contrasting thermophilization among European forests, grasslands and alpine summits

Kai Yue[1, 2, 3*], Pieter Vangansbeke[2, 4], Isla H. Myers-Smith[5], Donald M. Waller[6], Kris Verheyen[2], Markus Bernhardt-Römermann[7, 8, 9], Lander Baeten[2], Ingmar R. Staude[8], Anne D. Bjorkman[10], Radim Hédl[11, 12], Christopher Andrews[13], Elena Barni[14], Thomas Becker[15], Antoine Becker-Scarpitta[16], José-Luis Benito-Alonso[17], Jonathan Bennie[18], Imre Berki[19], Volker Blüml[20], Jörg Brunet[21], James M. Bullock[22], Hans Van Calster[4], Michele Carbognani[23], Markéta Chudomelová[11], Déborah Closset-Kopp[24], Pavel Dan Turtureanu[25], Gergana N. Daskalova[26], Guillaume Decocq[24], Jan Dick[13], Martin Diekmann[27], Thomas Dirnböck[28], Tomasz Durak[29], Ove Eriksson[30], Brigitta Erschbamer[31], Bente Jessen Graae[32], Thilo Heinken[33], Martin Hermy[34], Peter Horchler[35], Ute Jandt[7, 36], Bogdan Jaroszewicz[37], Róbert Kanka[38], Jozef Kollár[38], Martin Kopecký[39, 40], Thomas Kudernatsch[41], Andrea Lamprecht[42, 43], Jonathan Lenoir[24], Martin Macek[39], Marek Malicki[44, 45], František Máliš[46], Ottar Michelsen[47], Fraser Mitchell[48], Tobias Naaf[49], Thomas A. Nagel[50], Miles Newman[48], Adrian C. Newton[51], Lena Nicklas[31], Ludovica Oddi[14], Anna Orczewska[52], Simone Orsenigo[53], Adrienne Ortmann-Ajkai[54], Jan den Ouden[55], Harald Pauli[42, 43], George Peterken[56], Petr Petřík[39, 57], Remigiusz Pielech[58], Mihai Puşcaş[25, 59], Christophe Randin[60, 61, 62], Kamila Reczyńska[63], Christian Rixen[64, 65], Fride Høistad Schei[66], Wolfgang Schmidt[67], Jan Šebesta[68], Alina Stachurska-Swakon[58], Tibor Standovár[69], Krzysztof Świerkosz[70], Balázs Teleki[71], Jean-Paul Theurillat[61, 72], Tudor-Mihai Ursu[73], Thomas Vanneste[2], Mark Vellend[74], Philippine Vergeer[75], Ondřej Vild[11], Luis Villar[76], Pascal Vittoz[77], Manuela Winkler[42, 43], Sonja Wipf[64], Fuzhong Wu[1], Shengmin Zhang[2], Pieter De Frenne[2]

1. Key Laboratory for Humid Subtropical Eco-Geographical Processes of the Ministry of Education, School of Geographical Sciences, Fujian Normal University, Fuzhou, China
2. Forest & Nature Lab, Department of Environment, Ghent University, Melle-Gontrode, Belgium
3. Natural Resources Institute Finland (Luke), Helsinki, Finland
4. Research Institute for Nature and Forest, Brussels, Belgium
5. Department of Forest and Conservation Sciences, University of British Columbia, Vancouver, Canada
6. Department of Botany, University of Wisconsin, Madison, WI, USA
7. Institute of Biodiversity, Ecology and Evolution, Friedrich Schiller University Jena, Jena, Germany
8. German Centre for Integrative Biodiversity Research (iDiv) Halle-Jena Leipzig, Leipzig, Germany
9. Senckenberg Institute for Plant Form and Function Jena (SIP), Jena, Germany
10. Department of Biological and Environmental Sciences, University of Gothenburg, Gothenburg, Sweden
11. Institute of Botany, Czech Academy of Sciences, Brno, Czech Republic
12. Department of Botany, Faculty of Science, Palacký University in Olomouc, Czech Republic
13. UK Centre for Ecology and Hydrology, Penicuik, Midlothian, UK
14. Department of Life Sciences and Systems Biology, University of Turin, Turin, Italy
15. Geobotany, Regional and Environmental Sciences, University of Trier, Trier, Germany
16. CIRAD, UMR PVBMT, F-97410 St Pierre, La Réunion, France
17. GLORIA-Aragon Coordination, Jolube Consultor Botánico y Editor, Huesca, Spain
18. Centre for Geography and Environmental Science, Exeter University, Penryn, Cornwall, UK
19. Faculty of Forestry, University of Sopron, Sopron, Hungary
20. BMS-Umweltplanung, Osnabrück, Germany
21. Southern Swedish Forest Research Centre, Swedish University of Agricultural Sciences, Alnarp, Sweden
22. UK Centre for Ecology & Hydrology, Wallingford, UK

23. Department of Chemistry, Life Sciences and Environmental Sustainability, University of Parma, Parma, Italy
24. UMR CNRS 7058, “Ecologie et Dynamique des Systèmes Anthropisés” (EDYSAN), Université de Picardie Jules Verne, Amiens, France
25. A. Borza Botanic Garden, Babeș-Bolyai University, Cluj-Napoca, Romania
26. Department of Conservation Biology, University of Goettingen, Goettingen, Germany
27. Institute of Ecology, FB 2, University of Bremen, Bremen, Germany
28. Environment Agency Austria, Vienna, Austria
29. Faculty of Biology and Nature Protection, University of Rzeszów, Rzeszów, Poland
30. Department of Ecology, Environment and Plant Sciences, Stockholm University, Stockholm, Sweden
31. Department of Botany, University of Innsbruck, Innsbruck, Austria
32. Department of Biology, NTNU, Trondheim, Norway
33. Institute of Biochemistry and Biology, University of Potsdam, Potsdam, Germany
34. Division Forest, Nature and Landscape, University of Leuven, Leuven, Belgium
35. Department of Vegetation Studies and Landscape Management, Federal Institute of Hydrology, Koblenz, Germany
36. Department of Geobotany and Botanical Garden, Martin Luther University Halle-Wittenberg, Halle, Germany
37. Białowieża Geobotanical Station, Faculty of Biology, University of Warsaw, Białowieża, Poland
38. Institute of Landscape Ecology, Slovak Academy of Sciences, Bratislava, Slovakia
39. Institute of Botany of the Czech Academy of Sciences, Průhonice, Czech Republic
40. Faculty of Forestry and Wood Sciences, Czech University of Life Sciences Prague, Praha, Czech Republic

41. Bavarian State Institute of Forestry, Freising, Germany
42. GLORIA co-ordination, Institute for Interdisciplinary Mountain Research (ÖAW-IGF), Austrian Academy of Sciences, Vienna, Austria
43. GLORIA co-ordination, Institute of Botany, Department of Ecosystem Management, Climate and Biodiversity, BOKU University, Vienna, Austria
44. Department of Botany, Faculty of Biological Sciences, University of Wrocław, Wrocław, Poland
45. Botanical Garden of Medicinal Plants, Department of Pharmaceutical Biology and Biotechnology, Wrocław Medical University, Wrocław, Poland
46. Faculty of Forestry, Technical University in Zvolen, Zvolen, Slovakia
47. Department of Industrial Economics and Technology Management, Norwegian University of Science and Technology (NTNU), Trondheim, Norway
48. Botany Department and Trinity Centre for Biodiversity Research, School of Natural Sciences, Trinity College, University of Dublin, Dublin 2, Ireland
49. Leibniz Centre for Agricultural Landscape Research (ZALF), Muencheberg, Germany
50. Department of Forestry and Renewable Forest Resources, Biotechnical Faculty, University of Ljubljana, Ljubljana, Slovenia
51. Department of Life and Environmental Sciences, Bournemouth University, Poole, Dorset, UK
52. Faculty of Natural Sciences, Institute of Biology, Biotechnology and Environmental Protection, University of Silesia, Katowice, Poland
53. Department of Earth and Environmental Sciences, University of Pavia, Pavia, Italy
54. Department of Hydrobiology, Institute of Biology, University of Pécs, Pécs, Hungary
55. Forest Ecology and Forest Management Group, Wageningen University and Research Centre, Wageningen, the Netherlands

56. Beechwood House, Gloucestershire, UK
57. Faculty of Environmental Sciences, Czech University of Life Sciences, Prague, Czech Republic
58. Institute of Botany, Faculty of Biology, Jagiellonian University in Kraków, Poland
59. Department of Taxonomy and Ecology, Faculty of Biology and Geology, Babeș-Bolyai University, Cluj-Napoca, Romania
60. Department of Ecology and Evolution, University of Lausanne, Lausanne, Switzerland
61. Fondation du Jardin botanique Flore-Alpe, Champex-Lac, Switzerland
62. CIRM, Bramois, Switzerland
63. Independent Researcher, Wrocław, Poland
64. WSL Institute for Snow and Avalanche Research SLF, Davos, Switzerland
65. Climate Change, Extremes and Natural Hazards in Alpine Regions Research Centre CERC, Davos Dorf, Switzerland
66. Norwegian Institute of Bioeconomy Research, Bergen, Norway
67. Department of Silviculture and Forest Ecology of the Temperate Zones, University of Göttingen, Göttingen, Germany
68. Department of Forest Botany, Dendrology and Geobiocoenology, Faculty of Forestry and Wood Technology, Mendel University in Brno, Czech Republic
69. Department of Plant Systematics, Ecology and Theoretical Biology, ELTE Eötvös Loránd University, Budapest, Hungary
70. Museum of Natural History, University of Wrocław, Wrocław, Poland
71. Faculty of Cultural Sciences, Education and Regional Development, University of Pécs, Pecs, Hungary
72. Department of Plant Sciences, University of Geneva, Chambésy, Switzerland
73. Institute of Biological Research Cluj, National Institute of Research and Development for Biological

Sciences, Cluj-Napoca, Cluj County, Romania

74. Département de Biologie, Université de Sherbrooke, Sherbrooke, Québec, Canada

75. Plant Ecology and Nature Conservation Group, Wageningen University, Wageningen, the Netherlands

76. Instituto Pirenaico de Ecología, IPE-CSIC, Jaca, Huesca, Spain

77. Institute of Earth Surface Dynamics, Faculty of Geosciences and Environment, University of Lausanne, Lausanne, Switzerland

*Author for correspondence: kyleyuechina@163.com; kkyue@fjnu.edu.cn

Abstract

Climate warming is shifting biological communities, favouring warmth-demanding species at the expense of cold-adapted species in a process referred to as thermophilization[1-4]. Because biodiversity responses often lag behind climate warming, climatic debts are accumulating in many ecosystems across the globe[5-7]. While we might expect thermophilization and climatic debts to vary among habitats, standardized quantification across ecosystems is still lacking. Here we analysed multidecadal data from 6067 resurveyed vegetation plots over 12–78 years in forests, grasslands, and on alpine summits across Europe. We demonstrate that forest understory and grassland plant communities experienced positive thermophilization, although not significantly different from zero, whereas alpine summit vegetation showed much stronger (up to five times) and significant thermophilization. Thermophilization was driven largely by increases in warmth-demanding species in grasslands, by declines in cold-adapted species on alpine summits, and by both processes in forests. Significant climatic debts have accumulated in forests and alpine summits, but less so in grasslands, with debts positively correlated with macroclimate temperature changes. Our findings highlight divergent thermophilization trajectories and increasing debts across ecosystems. Further disentangling the mechanisms that allow some communities to track climate change more closely than others is critical to furthering our understanding of ecological resilience in a warming world.

Main

Global climate change is having profound impacts on biodiversity[8-10]. Range shifts are observed in many species and ecosystem types as species track their thermal requirements[11-14]. As a result, directional shifts in community composition at the expense of cold-adapted and in favour of warmth-demanding species (referred to as thermophilization) are increasingly evident in terrestrial and aquatic plant and animal communities[1-4,15,16]. For example, significant thermophilization of vegetation has been documented across alpine summits and grasslands in Europe[3,17], but also in plant communities of temperate and tropical forests despite the buffering effects of forest canopies[1,18-20]. However, the thermophilization rate of many biological communities is not keeping pace with the velocity of contemporary climate change[13,18,21,22], leading to a climatic lag or debt in community responses to climate warming[2,5,6,15,23].

Climatic debts reflect species' inherent life-history and ecophysiological characteristics such as limited dispersal and establishment capacity, as well as long life span[7,24,25], but may also arise from the buffering effects of microclimatic processes or interactions with other global change drivers[1,18,23,26]. Apparent debts may also be shaped by adaptive shifts in species' climatic niches, although such processes are generally slow[7]. Microclimates in unforested ecosystems, such as alpine summits and grasslands, are mainly shaped by topography and vegetation feedbacks on snow cover, solar radiation, air mixing, and evapotranspiration[27-30], while in forests, tree canopy structure, largely governs microclimatic conditions and thermal buffering[1,18], although topography would be also important[31]. As such, the magnitude of thermophilization might differ appreciably among ecosystems. However, comparing thermophilization studies is difficult, as they often employ different methodologies to quantify thermal niches and climatic debts (e.g.,

as a result of different sources, resolutions, seasons and base periods of climate data). While thermophilization rates in response to climate change may differ across ecosystems[4], to date, we lack consistent large-scale, multi-taxa, and long-term comparisons of rates of thermophilization and magnitudes of climatic debt among vegetation types based on a consistent methodology. To address this knowledge gap, we here used vegetation resurveys with a consistent methodology to answer two key questions: (1) how do thermophilization rates and climatic debts differ among different ecosystems types, and (2) how are these differences related to variation in local climate warming across contrasting ecosystems?

Here we report cross-biome thermophilization for Europe's temperate forests, grasslands and alpine summits, which represent widespread and ecologically distinct vegetation types with contrasting structure and microclimate relevant to species' responses to climate change. To this end, we compiled plant occurrence data for 1919 species from 6067 resurveyed vegetation plots (Fig. 1). In each plot, we quantified the thermophilization rate of the plant community[1,18] using a consistent methodology (see Methods). In total, we used 4372, 1209, and 486 plots from forests, grasslands, and alpine summits, respectively, with the sampling intervals (baseline to resurveys) of 12 to 78 (median 42), 16 to 78 (median 35), and 12 to 15 (median 14) years, respectively (Extended Data Fig. 1a, Table 1). We use these data to estimate rates of thermophilization and climatic debt (°C decade^{-1}) for each plot using an established method that relies on species' thermal affinities inferred from their geographic distributions relative to long-term climate data[1,18,32]. To further disentangle the mechanisms underlying thermophilization, we separately calculated changes in the 5th and 95th percentiles of the floristic temperature distribution to represent declines of cold-adapted *vs.* increases of warmth-

189 demanding species, respectively[1].

190

191 When estimated using plant abundance data (excluding rare species with range sizes fewer than
192 1000 grid cells in 20 × 20 km resolution; see Methods), which mainly reflect changes in species
193 dominance and community reordering, we found positive, although not significantly different
194 from zero, rates of overall thermophilization in forests [0.03 °C decade^{-1}, 95% credible interval
195 (CI): -0.02–0.07] and grasslands [0.03 °C decade^{-1}, 95% CI: -0.06–0.11], while the overall
196 thermophilization rate on alpine summits was much higher and significantly different from zero
197 at 0.12 °C decade^{-1} (95% CI: 0.05–0.19) (Fig. 2a). When estimated using plant
198 presence/absence data, which are more sensitive to species turnover including rare or transient
199 species, similar results were found, and thermophilization rate on alpine summits was five times
200 higher than in forests and grasslands (Extended Data Fig. 2a; see Sensitivity analysis). When
201 assessed using abundance data and excluding rare species, thermophilization in grasslands was
202 driven largely by increase in warmth-demanding species (0.08 °C decade^{-1}, 95% CI: -0.03–
203 0.19). In forests, thermophilization reflected both declines in cold-adapted species (0.04, 95%
204 CI: -0.01–0.09 °C decade^{-1}) and increases in warmth-demanding species (0.03, 95% CI: -0.03–
205 0.09 °C decade^{-1}). On alpine summits, however, we found a significant decrease in cold-adapted
206 species (0.26 °C decade^{-1}, 95% CI: 0.18–0.34) and a decrease in warmth-demanding species (-
207 0.16 °C decade^{-1}, 95% CI: -0.25 – -0.06). These trends did not show marked changes when
208 assessed including rare species and/or using vegetation presence/absence data (Extended Data
209 Fig. 2b; see Sensitivity analysis).

210

211 Our second analysis calculated climatic debts by subtracting rates of thermophilization from

local rates of climate change[2,24]. These climatic debts were mostly positive (ranging from 0.13 to 0.34 °C decade^{-1} across ecosystem types; Fig. 2b, Extended Data Fig. 2), indicating that thermophilization lags behind macroclimate changes. The magnitude of these lags did not strongly depend on whether they were estimated from declines in cold-adapted species, increases in warmth-demanding species, or overall thermophilization rates. Climatic debts were generally highest in forests, followed by alpine summits, and were lowest in grasslands. Thermophilization rates were weakly correlated with rates of increase in temperature regardless of the ecosystem type, while climatic debts strongly covaried with rates of temperature change across all ecosystem types (Fig. 3).

The overall rates of thermophilization on alpine summits were generally higher, up to five times, than those in forests and grasslands. Divergence in thermophilization rates between ecosystem types may be attributed, at least partially, to differences in plant lifespans, with communities composed of shorter-lived plants potentially responding more rapidly to climate warming[33,34]. However, currently available lifespan datasets (e.g., from the TRY Plant Trait Database[35]) are still limited in taxonomic coverage and resolution, especially for ecosystems such as alpine summits and forests where many plant species are known to have extremely long lifespans, preventing us from quantitatively testing this hypothesis. The high thermophilization observed on alpine summits may particularly result from the rugged topography that compresses thermal belts, creating strong spatial gradients in microclimate and species composition, such that even small shifts in species distribution can lead to marked community-level changes in thermal affinity[36], especially above the forest belt, where climatic buffering through tree canopies is absent. Within the alpine summit dataset, however, we did not detect significant relationships

between thermophilization rates and variables reflecting rugged topography such as the terrain ruggedness index (TRI) or slope (Extended Data Fig. 3a), probably because the summit-level coordinates in our database and mid-scale topographic metrics fail to capture the fine-scale microhabitats that more strongly shape community responses, especially in alpine environments. Nevertheless, we found that thermophilization was lowest on north-facing slopes (Extended Data Fig. 3b), which can support the hypothesis of microhabitats generated by rugged topographic gradients and emphasize the role of slope exposition to sun radiation in shaping thermophilization patterns of treeless alpine vegetation.

Our results further suggest that thermophilization of understory plants in forests was driven by both declines in cold-adapted species and increases in warmth-demanding species, which is expected with warming. By contrast, only increases in warmth-demanding species contributed to the overall thermophilization in grasslands. Unlike forests, grasslands lack tree canopy buffering, and grassland plant communities experience hotter maximum daily temperatures than forest understoreys. Together with higher species turnover and recruitment rates, this could have favoured warmth-demanding taxa more as temperatures raise[37], resulting in thermophilization being driven mainly by increases in warmth-demanding species. For alpine summits, however, our results suggest a simultaneous decline of both cold-adapted and warmth-demanding species, which could potentially be linked to recurring severe drought during the survey periods[38,39], although likely reflecting additionally distinct ecological pressures. Cold-adapted species may be lost due to pronounced climate warming and habitat contraction[40,41], while the decline of warmth-demanding species may result from reduced persistence after colonization, possibly due to environmental stress or biotic interactions[42]. Despite declines in

both types of species, net thermophilization can still result from stronger declines in cold-adapted species than warmth-demanding species (Fig. 2, Extended Data Fig. 2), as well as from compositional shifts favouring warmth-demanding species, through both topography-facilitated colonization and differential persistence[43]. By partitioning thermophilization into the effects of gains, losses, and abundance shifts of persisting species, we found that abundance shifts, along with losses, were the primary drivers of thermophilization on alpine summits (Extended Data Fig. 4a; see Sensitivity analysis). Results also confirmed that thermophilization was jointly driven by losses in cold-adapted species and gains in warmth-demanding species in forests and largely by gains in warmth-demanding species in grasslands.

Substantial climatic debts exist in all the types of ecosystems studied here. Climatic debts in forests were substantial and generally higher than those in alpine summits and grasslands. This is likely because tree canopies provide microclimatic buffering of climate warming, which is not captured by the macroclimate data used to assess global climate warming (and in our study)[23,44]. Also, forest plant life-history traits (e.g., long lifespan) likely impede their ability to adapt rapidly to changing conditions, delaying their response and increasing their climatic debt[6,45]. The lower climatic debt in grasslands indicates that shifts in grassland plant communities are more closely tracking climate warming[37], especially for warmth-demanding species that showed limited climatic debts. Furthermore, we quantified the thermal suitability of the background climate for plant communities and assessed the extent to which species at the plot level were exposed to climatic conditions beyond their thermal tolerance ranges (see Sensitivity analysis for details). We found significant declines in the probability density of thermal suitability in forests and marginal declines in grasslands, but not on alpine summits

(Extended Data Fig. 5a). The proportion of mismatched species significantly increased in forests, but not in grasslands or alpine summits (Extended Data Fig. 5b). These results highlight that thermal mismatch progresses unevenly across ecosystems, and that comparing the difference between changes in climate and floristic temperature may have overestimated climatic debts in grasslands and alpine summits. Importantly, disturbance levels among ecosystems could also contribute to these differences; although we were unable to assess this factor with the current data, it represents a significant direction for future research. Together, these results emphasize the ecosystem-specific responses of vegetation to climate warming.

In addition, our results that climatic debts increase with the amount of temperature change suggest that rapid climate change increases the risk of species reshuffling and ecosystem disruptions[5,7]. This highlights the urgency of proactive strategies to mitigate and adapt to future climate change. As physical and biological drivers of microclimate are very different in forests, grasslands and alpine summits[46], future research should quantify how climatic debt scales with different rates of warming in each of these contrasting habitats. In addition to climate warming, other global change factors such as droughts, nitrogen and sulfur deposition, land use change, and elevated CO_2, may interact with or modulate thermophilization patterns[14,47]. Part of the thermophilization signal we detect might be due to niche axes that are correlated with, but not causally linked to, temperature. Multi-factor assessments, including other global environmental changes, are thus needed to more precisely predict the responses of plant communities and inform more integrative conservation strategies.

In sum, we uncovered the novel finding that thermophilization rates vary significantly between

major habitat types – forests, grasslands, and alpine summits – in Europe. Thermophilization was driven largely by increases in warmth-demanding species in grasslands, by decrease in cold-adapted and increases in warmth-demanding species in forests, and by decreases in cold-adapted species, as well as abundance shifts of persisting species, on alpine summits. Although time lags between the climate warming and changes in the composition of plant communities have been previously noted[6,7,12,18,48,49], we here find that climate change has generated contrasting shifts in plant communities among different ecosystem types. These contrasting patterns suggest asynchronous reorganization among ecosystems, reflecting differences in exposure, biotic resistance, and response lags. Importantly, ecosystems with accumulating climatic debts likely face elevated risks of ecological mismatches, functional instability, and local species extirpations. Given rapid rates of climate change, climate lags will likely persist over many decades even if the climatic debt must ultimately be paid off. The differing thermophilization rates among ecosystems also highlight the importance of comparing several ecosystems when assessing the impacts of global change on biodiversity, as such quantification can permit forecasting of the duration of biodiversity changes that will continue even if climate warming stabilizes. Our findings facilitate the development of targeted management strategies, such as assisted migration in forests, adaptive grazing practices in grasslands, and conservation of cold-adapted species where possible while enabling the establishment of warmth-demanding species on alpine summits, to enhance ecosystem resilience and mitigate biodiversity loss under ongoing climate change.

Online content

Any methods, additional references, Nature Portfolio reporting summaries, source data,

extended data, supplementary information, acknowledgements, peer review information; details of author contributions and competing interests; and statements of data and code availability are available at…

References

1 De Frenne, P. *et al.* Microclimate moderates plant responses to macroclimate warming. *Proceedings of the National Academy of Sciences* **110**, 18561-18565 (2013).

2 Fadrique, B. *et al.* Widespread but heterogeneous responses of Andean forests to climate change. *Nature* **564**, 207-212 (2018).

3 Gottfried, M. *et al.* Continent-wide response of mountain vegetation to climate change. *Nature Climate Change* **2**, 111-115, doi:10.1038/nclimate1329 (2012).

4 Khaliq, I. *et al.* Warming underpins community turnover in temperate freshwater and terrestrial communities. *Nature Communications* **15**, 1921 (2024).

5 Alexander, J. M. *et al.* Lags in the response of mountain plant communities to climate change. *Global Change Biology* **24**, 563-579, doi:https://doi.org/10.1111/gcb.13976 (2018).

6 Bertrand, R. *et al.* Changes in plant community composition lag behind climate warming in lowland forests. *Nature* **479**, 517-520, doi:10.1038/nature10548 (2011).

7 Svenning, J. C. & Sandel, B. Disequilibrium vegetation dynamics under future climate change. *American Journal of Botany* **100**, 1266-1286 (2013).

8 Parmesan, C. Ecological and evolutionary responses to recent climate change. *Annual Review of Ecology, Evolution, and Systematics* **37**, 637-669 (2006).

9 Pecl, G. T. *et al.* Biodiversity redistribution under climate change: Impacts on ecosystems and human well-being. *Science* **355**, eaai9214 (2017).

10 Scheffers, B. R. *et al.* The broad footprint of climate change from genes to biomes to people. *Science* **354**, aaf7671 (2016).

11 Chen, I.-C., Hill, J. K., Ohlemüller, R., Roy, D. B. & Thomas, C. D. Rapid range shifts of species associated with high levels of climate warming. *Science* **333**, 1024-1026, doi:doi:10.1126/science.1206432 (2011).

12 Lenoir, J. & Svenning, J.-C. Climate-related range shifts – a global multidimensional synthesis and new research directions. *Ecography* **38**, 15-28, doi:https://doi.org/10.1111/ecog.00967 (2015).

13 Lenoir, J. *et al.* Species better track climate warming in the oceans than on land. *Nature Ecology & Evolution* **4**, 1044-1059 (2020).

14 Sanczuk, P. *et al.* Unexpected westward range shifts in European forest plants link to nitrogen deposition. *Science* **386**, 193-198, doi:doi:10.1126/science.ado0878 (2024).

15 Devictor, V. *et al.* Differences in the climatic debts of birds and butterflies at a continental scale. *Nature Climate Change* **2**, 121-124, doi:10.1038/nclimate1347 (2012).

16 Stuart-Smith, R. D., Edgar, G. J., Barrett, N. S., Kininmonth, S. J. & Bates, A. E. Thermal biases and vulnerability to warming in the world's marine fauna. *Nature* **528**, 88-92, doi:10.1038/nature16144 (2015).

17 Vanneste, T. *et al.* Impact of climate change on alpine vegetation of mountain summits in Norway. *Ecological Research* **32**, 579-593, doi:https://doi.org/10.1007/s11284-017-1472-1 (2017).

18 Zellweger, F. *et al.* Forest microclimate dynamics drive plant responses to warming. *Science* **368**, 772-775 (2020).

19 De Frenne, P. *et al.* Global buffering of temperatures under forest canopies. *Nature Ecology & Evolution* **3**, 744-749, doi:10.1038/s41559-019-0842-1 (2019).

20 Duque, A., Stevenson, P. R. & Feeley, K. J. Thermophilization of adult and juvenile tree communities in the northern tropical Andes. *Proceedings of the National Academy of Sciences* **112**, 10744-10749, doi:doi:10.1073/pnas.1506570112 (2015).

21 Ash, J. D., Givnish, T. J. & Waller, D. M. Tracking lags in historical plant species' shifts in relation to regional climate change. *Global Change Biology* **23**, 1305-1315, doi:https://doi.org/10.1111/gcb.13429 (2017).

22 Burrows, M. T. *et al.* The Pace of Shifting Climate in Marine and Terrestrial Ecosystems. *Science* **334**, 652-655, doi:doi:10.1126/science.1210288 (2011).

23 Richard, B. *et al.* The climatic debt is growing in the understorey of temperate forests: Stand characteristics matter. *Global Ecology and Biogeography* **30**, 1474-1487, doi:https://doi.org/10.1111/geb.13312 (2021).

24 Bertrand, R. *et al.* Ecological constraints increase the climatic debt in forests. *Nature Communications* **7**, 12643 (2016).

25 Laughlin, D. C. & McGill, B. J. Trees have overlapping potential niches that extend beyond their realized niches. *Science* **385**, 75-80, doi:doi:10.1126/science.adm8671 (2024).

26 Govaert, S. *et al.* Rapid thermophilization of understorey plant communities in a 9 year-long temperate forest experiment. *Journal of Ecology* **109**, 2434-2447, doi:https://doi.org/10.1111/1365-2745.13653 (2021).

27 Bernath-Plaisted, J. S., Ribic, C. A., Hills, W. B., Townsend, P. A. & Zuckerberg, B. Microclimate complexity in temperate grasslands: implications for conservation and management under climate change. *Environmental Research Letters* **18**, 064023, doi:10.1088/1748-9326/acd4d3 (2023).

28 Geiger, R., Aron, R. H. & Todhunter, P. *The climate near the ground*. (Rowman & Littlefield, 2009).

29 Potter, K. A., Arthur Woods, H. & Pincebourde, S. Microclimatic challenges in global change biology. *Global Change Biology* **19**, 2932-2939 (2013).

30 Aalto, J., Scherrer, D., Lenoir, J., Guisan, A. & Luoto, M. Biogeophysical controls on soil-atmosphere thermal differences: implications on warming Arctic ecosystems. *Environmental Research Letters* **13**, 074003 (2018).

31 Borderieux, J. *et al.* Cool topoclimates promote cold-adapted plant diversity in temperate mountain forests. *Peer Community Journal* **5**, doi:10.24072/pcjournal.519 (2025).

32 Vangansbeke, P. *et al.* ClimPlant: Realized climatic niches of vascular plants in European forest understoreys. *Global Ecology and Biogeography* **30**, 1183-1190 (2021).

33 Compagnoni, A. *et al.* Herbaceous perennial plants with short generation time have stronger responses to climate anomalies than those with longer generation time. *Nature Communications* **12**, 1824, doi:10.1038/s41467-021-21977-9 (2021).

34 Poppenwimer, T., Mayrose, I. & DeMalach, N. Revising the global biogeography of annual and perennial plants. *Nature* **624**, 109-114, doi:10.1038/s41586-023-06644-x (2023).

35 Kattge, J. *et al.* TRY plant trait database–enhanced coverage and open access. *Global Change Biology* **26**, 119-188 (2020).

36 Steinbauer, M. J. *et al.* Accelerated increase in plant species richness on mountain summits is linked to warming. *Nature* **556**, 231-234, doi:10.1038/s41586-018-0005-6 (2018).

37 Zhu, K. *et al.* Rapid shifts in grassland communities driven by climate change. *Nature Ecology & Evolution*, doi:10.1038/s41559-024-02552-z (2024).

38 Mayo de la Iglesia, R. *et al.* Divergent responses of alpine bryophytes and lichens to climate change

in the Swiss Alps. *Journal of Vegetation Science* **35**, e13292 (2024).

39 Vorkauf, M., Kahmen, A., Körner, C. & Hiltbrunner, E. Flowering phenology in alpine grassland strongly responds to shifts in snowmelt but weakly to summer drought. *Alpine Botany* **131**, 73-88 (2021).

40 Rumpf, S. B. *et al.* Extinction debts and colonization credits of non-forest plants in the European Alps. *Nature Communications* **10**, 4293 (2019).

41 Steinbauer, K., Lamprecht, A., Semenchuk, P., Winkler, M. & Pauli, H. Dieback and expansions: species-specific responses during 20 years of amplified warming in the high Alps. *Alpine Botany* **130**, 1-11, doi:10.1007/s00035-019-00230-6 (2020).

42 Alexander, J. M., Diez, J. M. & Levine, J. M. Novel competitors shape species' responses to climate change. *Nature* **525**, 515-518, doi:10.1038/nature14952 (2015).

43 García Criado, M. *et al.* Plant diversity dynamics over space and time in a warming Arctic. *Nature*, doi:10.1038/s41586-025-08946-8 (2025).

44 Chen, S. *et al.* Macroclimate and canopy characteristics regulate forest understory microclimatic temperature offsets across China. *Global Ecology and Biogeography* **33**, e13830, doi:https://doi.org/10.1111/geb.13830 (2024).

45 Thuiller, W., Lavorel, S., Araújo, M. B., Sykes, M. T. & Prentice, I. C. Climate change threats to plant diversity in Europe. *Proceedings of the National Academy of Sciences* **102**, 8245-8250 (2005).

46 De Frenne, P. *et al.* Ten practical guidelines for microclimate research in terrestrial ecosystems. *Methods in Ecology and Evolution* **16**, 269-294, doi:https://doi.org/10.1111/2041-210X.14476 (2025).

47 Brookshire, E. N. J. & Weaver, T. Long-term decline in grassland productivity driven by increasing dryness. *Nature Communications* **6**, 7148, doi:10.1038/ncomms8148 (2015).

48 Doak, D. F. & Morris, W. F. Demographic compensation and tipping points in climate-induced range shifts. *Nature* **467**, 959-962 (2010).

49 Lenoir, J., Gégout, J.-C., Marquet, P. A., de Ruffray, P. & Brisse, H. A significant upward shift in plant species optimum elevation during the 20th century. *Science* **320**, 1768-1771 (2008).

Main Text Figure Legends

Fig. 1 | Distribution of the 6067 resurveyed (quasi-)permanent plots in forests, grasslands

and alpine summits across Europe. Forest cover (green) and grassland cover (yellow) are based on CORINE Land Cover 2018 data (© European Environment Agency, 2018), and elevation data (gray) are from the Shuttle Radar Topography Mission (SRTM, courtesy of NASA/USGS).

Fig. 2 | Vegetation thermophilization rates and climatic debts (°C decade^{-1}) in forests, grasslands, and alpine summits. a, Vegetation thermophilization rates quantified as the declines in cold-adapted species (5th percentile shift), overall (median shift), and increases of warmth-demanding species (95th percentile shift). **b,** Climatic debts calculated according to climate change rates and vegetation thermophilization rates of decline in cold-adapted species, overall, and increase of warmth-demanding species. Thermophilization rates and climatic debts were estimated using plant abundance data excluding rare species. Circles represent means (n = 4372, 1209, and 457 plots for forests, grasslands, and alpine summits, respectively) with 80% (thick line) and 95% (thin line) credible intervals and posterior distributions obtained from Bayesian mixed-effects models.

Fig. 3 | Relationships between vegetation thermophilization rate/climatic debt and the growing season mean temperature (T_{mean}) change rate in forests, grasslands, and alpine summits. a-c, Relationships between growing season T_{mean} change rate (°C decade^{-1}) and thermophilization rate (°C decade^{-1}) quantified as the declines of cold-adapted species (5th percentile shift), overall (median shift), and increases of warmth-demanding species (95th percentile shift). **d-f,** Relationships between growing season T_{mean} change rate (°C decade^{-1}) and climatic debt (°C decade^{-1}) calculated according to thermophilization rate quantified as the declines of cold-adapted species, overall, and increases of warmth-demanding species. Thermophilization rates and climatic debts were estimated using plant abundance data excluding rare species. Each circle represents a plot (n = 4372, 1209, and 457 for forests, grasslands, and alpine summits, respectively). Lines are fits from Bayesian mixed-effect models, and shaded areas denote 95% credible intervals.

Methods

Databases and vegetation resurveys

We used data from three databases, and each database is a collation of vegetation resurvey data for a certain ecosystem type in Europe (Fig. 1, Extended Data Table 1). Data for forests were obtained from the forestREplot database version 2.3 (www.forestreplot.ugent.be) with 4372 plots from 76 sampling sites. The forestREplot is a resurveyed vegetation plot network focusing on all vascular plants in the understory community (<1 m height, including tree seedlings) across temperate forests in Europe[50], as they represent on average the most important plant biodiversity compartment in forests[51]. All plots are located in natural (never cleared for other land uses than forests according to the oldest available sources such as historical maps, typically at least 150-300 years[52]) or semi-natural forests according to the definition by Peterken[53]. Grasslands were represented by 1209 resurveyed vegetation plots from 22 sites that are situated in semi-natural grasslands, which is defined as unploughed mown or grazed areas with limited fertilization[54], from the GRACE database[55]. Data for alpine summits were from the Global Observation Research Initiative in Alpine environments (GLORIA, https://gloria.ac.at) with 486 plots in natural vegetation with a complete list of vascular plant species from 64 sites[56]. In each site, plant communities were surveyed across permanent (i.e., plots were permanently marked in the field) or quasi-permanent (i.e., plots were not permanently marked but have known coordinates or clear indications on physical maps for later accurate relocation)[57] plots at two time points, namely the baseline survey and resurvey. Between the two surveys, there was no major change in land use such as clearcutting, replanting, conversion to agricultural land or urbanization, etc., and, at least at the plot level, the same methodology was used in both surveys, such as number and size of plots and cover-abundance scale (for more details see

497 references[50,55,56]). The time spans between baseline survey and resurvey ranged between 12 and
498 78 years with a median of 42 years. Specific lengths of the study period per ecosystem type are
499 available in Extended Data Table 1. The median number of plots per site was 42.5 and 39 in
500 forest and grassland surveys, respectively, and the median size of plots was 200 and 25 m^2 in
501 forest and grassland surveys, respectively[58]. Alpine summits were always resurveyed in eight
502 spatial sections that together covered the entire area from the highest summit point to the
503 contour line 10 m in elevation below this point, and the median summit area was around 300
504 m^2. A complete list of vascular plant species was recorded for all plots in each ecosystem type.
505 Species abundance was recorded as percentage cover in forest and grassland plots, and as an
506 ordinal scale from one (very rare) to eight (dominant) in summit plots[56]. The ordinal abundance
507 scores were standardized for each plot and survey time to a continuous 0–100 scale via min-
508 max transformation, and subsequently converted to relative abundances, thereby rendering
509 them directly comparable to percentage cover estimates. Vegetation surveys were generally
510 carried out during the peak of the vegetation season (May–August), and plots with a year
511 difference between baseline survey and resurvey less than 10 year were excluded in our study.
512
513 **Temperature data**
514 To determine the rate of temperature change between the baseline survey and resurvey, we used
515 monthly mean temperature data to obtain mean growing season (April to September)
516 temperatures, given that this period broadly corresponds to the peak of plant physiological
517 activity, although on alpine summits this period is shorter (June to August), thereby better
518 reflecting the climatic condition driving species turnover and community dynamics[1,3,59,60]. We
519 used the data of CRU TS version 4.07, which provides updated gridded climate datasets at a

spatial resolution of 0.5° (~50 km at the equator) since 1901, based on monthly observations at meteorological stations across the world's land areas. This dataset was selected because of its temporal depth and consistency, allowing robust estimation of temperature change over the full period between baseline survey and resurvey (from 1931 to 2020). For each plot across the ecosystem types, we calculated climatic temperature change rate (expressed in °C decade^{-1}) between the baseline survey and the resurvey as the difference between the mean growing season temperature during the five years preceding the baseline survey and the five years preceding the resurvey, divided by the time span between the baseline survey and the resurvey[1,3,18]. The resulting distributions of mean growing season temperature change rates are presented in Extended Data Fig. 1b.

Thermophilization

To calculate thermophilization rates, we followed established and widely used methods in the literature based on species' thermal niche and distribution range data[1,3,6,15,18,20,61]. First, we extracted gridded long-term (1970-2000) climatic data on monthly mean temperature of the growing season (April to September) from WorldClim v.2 as a raster file with 10 arc-min resolution (~20 × 20 km)[62]. Then, to obtain distribution data of the species, we estimated species range sizes as area of occupancy (AOO)[63] using point occurrence records in the Global Biodiversity Information Facility (GBIF, www.gbif.org)[64]. We retained records from 1930 onward to ensure full temporal coverage of species' distributions across baseline survey and resurvey intervals, the earliest of which began in 1931 (see Extended Data Table 1). To minimize spatial sampling bias, occurrences were aggregated to 20 × 20 km resolution, and AOO was calculated based on the number of unique occupied grid cells per species, thereby

not only avoiding overrepresentation of well-sampled areas but also aligning with the resolution of the used climate data. Records with missing or erroneous coordinates, high spatial uncertainty (>10 km), or flagged as outliers were removed using standard data cleaning procedures. After filtering, a total of 1919 species (85.8%) out of the 2237 species identified to species level included in our study across ecosystem types were matched and retained. This GBIF-derived range sizes for plant species in Europe has been found to correlate strongly with expert-drawn range maps, and can thus provide good relative estimates of species' distributions[58,65]. Next, to estimate the realized thermal niches of species, defined as the climatic niche space that is genuinely occupied by a species[64], we set the study area extent to all European land between 15° W and 60° E and 25° N and 75° N, with grid cells of 20 × 20 km. For each species, we randomly sampled 1000 grid cells, with replacement, within the range size represented by AOO[18,32]. To generate consistent data series for all species (1000 values), we used random sampling with replacement instead of a random sample or all grid cells, which allowed species with small distribution ranges (i.e., <1000 grid cells) to be included under the same sampling scheme and ensured comparability of climatic niche estimates across species. However, because rare species (defined here as species with range sizes smaller than 1000 grid cells, which accounted for 36.4% of the total species pool; Extended Data Fig. 1c) are less frequently encountered, sampling efforts may not consistently detect them and thus lead to potential underestimation or overestimation of their actual contribution to thermophilization of vegetation communities. We thus first estimated themophilization rate and climatic debt only with species having AOO ≥ 1000 grid cells, and then reran the analyses with all the species included in our database to check if the exclusion of rare species has biased our results (see Sensitivity analysis).

We calculated the floristic temperature (T_{plant}, °C) for each plot by using the thermal niches of all species present during each survey (baseline survey and resurvey). To account for the variability and uncertainty in species' thermal preferences and niche widths, we generated the distribution of plot-level floristic temperatures at each survey by resampling 1000 times from the species' thermal niches (i.e., from the 1000 grid cells), with weights defined by species abundance, following the methodology explained in Rodríguez-Sánchez et al.[66]. Then, we estimated the overall thermophilization rate for each plot as the difference between the median of the floristic temperature distribution of the resurvey minus the baseline survey (ΔT_{plant}), divided by the time span (Δt, in decades) between the two survey periods. Given that thermophilization represents a slow ecological response to climate warming, we thus used decadal rates (°C decade^{-1}) in this study to better reflect long-term trends and reduce sensitivity to interannual variability. A positive value thus reflects an overall temporal increase of floristic temperature in °C decade^{-1}. To further evaluate the contribution of declines of cold-adapted species and increases of warmth-demanding species to the overall thermophilization rate, we also quantified shifts in the left (fifth percentile) and right (95th percentile) tails of the plot-level distribution of floristic temperatures per survey period, respectively[1]. Then, a positive value in the left versus right tail shift indicates thermophilization due to a decline of relatively cold-adapted versus an increase of the frequency of more warmth-demanding species, respectively. Since we were specifically interested in this per-plot thermophilization, it is important to note that this calculation of shifts in the cold-adapted *vs.* warmth-demanding species is a per-plot relative quantification based on the left and right tail of floristic temperature distribution shifts per plot[1]. As a result, a cold-adapted species in a plot in a warm site can be a warmth-demanding

589 species in a plot in a colder site. Finally, as a sensitivity analysis, we also converted all
590 vegetation data into presence/absence data and recalculated thermophilization rates and
591 climatic debt (see Sensitivity analyses).
592
593 **Climatic debt**
594 Climatic debt is defined as the degree to which the rates of compositional changes in vegetation
595 are lagging behind the rates of climate warming. The climatic debt per plot between the baseline
596 survey and resurvey was calculated as $(\Delta T_{clim}/\Delta t) - (\Delta T_{plant}/\Delta t)$ (following refs.[2,24]), where
597 ΔT_{clim} and ΔT_{plant} were changes in actual mean climate temperature of the growing season and
598 floristic temperature (the median, fifth and 95th percentile of the distribution of floristic
599 temperatures) between the baseline survey and resurvey, respectively. A large climatic debt
600 suggests a large mismatch between the dynamics of plant communities and climate change[7],
601 which indicates that a relatively large number of species are occurring under sub-optimal
602 thermal conditions. Positive (negative) climatic debts indicate that the response rates of plant
603 communities are slower (faster) than climate warming rates, respectively.
604
605 **Statistical analyses**
606 We used Bayesian mixed-effects models with the *brms* package[67] in R for all the statistical
607 analyses, and the 95% credible interval (CI) to determine statistical clarity[68]. We adopted a
608 Gaussian regression model with an identity link to evaluate whether thermophilization
609 rates/climatic debts (°C decade^{-1}) were significantly different from zero within each type of
610 ecosystem by fitting ecosystem type as a fixed-effect factor and "site" as a random-effect term.
611 The suitability of Gaussian assumption was evaluated using quantile-quantile (QQ) plots of the

response variables, which indicated approximate normality (Extended Data Fig. 6). Also, to account for the potential impacts of regression to the mean (RTM) effects[69], we included the mean climate temperature of the growing season at the baseline survey ($T_{clim_baseline}$) as a covariate, given the detected significant linear relationship between $T_{clim_baseline}$ and temperature change rate (Extended Data Fig. 7a). This approach helps separate baseline effect from true temporal trends. In addition, we also fitted plot size as a fixed-effects factor in the model, which was specified as the following formula (model 1):

$$\text{thermophilization rate/climatic debt} \sim \text{ecosystem_type} + \text{plot_size} + T_{clim_baseline} + (1|\text{site})$$

Then, to assess the relationships between actual climatic temperature change rate and the thermophilization rate/climatic debt based on vegetation surveys across ecosystem types, we fitted the interaction of actual climatic temperature change rate and ecosystem type as fixed-effects factors (model 2):

$$\text{thermophilization rate/climatic debt} \sim \Delta T_{clim} * \text{ecosystem_type} + \text{plot_size} + T_{clim_baseline} + (1|\text{site})$$

For each model, we fitted four chains of 8000 iterations, excluding the first 2000 iterations as warmup in each chain. We used Gelman-Rubin statistic ($\hat{R} < 1.01$) to ensure model convergence, and all the models in our analyses converged.

Sensitivity analyses

Thermophilization was primarily estimated using abundance-weighted data, which emphasize

635 shifts in community structure by giving more weight to dominant species. This approach
636 provides insights into changes in ecological dominance and potential functional consequences.
637 However, it may also underrepresent the role of rare or newly colonizing species, which can be
638 important indicators of climate-driven species turnover, and also bias the results because of
639 methodological and observer differences in abundance measurement. To address these
640 limitations and assess the robustness of our findings, we thus converted all abundance data into
641 robust presence/absence data following previous studies[1,18], and reran the analyses for the
642 estimation of thermophilization rate and climatic debt. This complementary approach captures
643 changes in species composition regardless of abundance, allowing for a more comprehensive
644 assessment of community thermal shifts. The rationale for performing this analysis lies in that
645 the time intervals between the baseline surveys and resurveys were mostly long enough (all >10
646 years) to allow for species replacements due to colonization and extinction. We found similar
647 results of thermophilization rate and climatic debt generated from vegetation abundance-
648 weighted and presence/absence data (Extended Data Fig. 2).
649
650 Rare species with small range sizes are often ecological outliers with unique habitat
651 requirements and thermal tolerances, and their presence may thus disproportionately influence
652 the calculation of average thermal preferences of plant community[70]. Also, rare species are less
653 likely to be consistently detected across sampling events due to their low abundance, and this
654 variability in detection can introduce noise into the data, making it difficult to accurately assess
655 trends in species composition over time[71]. We thus excluded rare species with AOO < 1000 grid
656 cells in our analyses. However, rare species themselves are important component of vegetation
657 community, and can be important indicators of climate-driven species turnover. Therefore, to

test if the exclusion of rare species in our analyses may affect the estimation of thermophilization rate and climatic debt, we reran such analyses by including all the species in our dataset. Results showed that the inclusion of rare species did not impact the overall patterns of thermophilization rates and climatic debts across all ecosystems (Extended Data Fig. 2b), indicating that the observed patterns are not an artifact of sampling bias toward rare taxa and reflect consistent community-level responses to climate warming.

In our study, we classified cold-adapted and warmth-demanding species based on the lower and upper 5% percentiles of the floristic temperature distribution. While this approach focused on species at the thermal distribution margins, it may also result in relatively small groups that are sensitive to outliers or sampling variation. To evaluate whether our results were disproportionately influenced by these few extreme cases, we conducted a sensitivity analysis using the lower and upper 20% percentiles of the floristic temperature distribution to define cold-adapted and warmth-demanding species, respectively. The results were consistent with our original findings, showing similar patterns in the direction of thermophilization responses across ecosystems (Extended Data Fig. 7b). However, the magnitude of the effects was slightly attenuated, as expected, due to the inclusion of species closer to the median of floristic temperature distribution. These results confirm that our conclusions are robust to the choice of quantile thresholds used to define thermal adaptation.

As a supplementary analysis for the method used to quantify the contributions of shifts in cold-adapted *vs.* warmth-demanding species to thermophilization, we further partitioned the observed changes in community-weighted, at the plot level, mean temperature (ΔT_{CWM}, °C)

into three additive components, namely species gains, species losses, and abundance shifts of persisting species[40,72]. This framework allows us to attribute community-level floristic temperature change into different forms of species turnover and reassembly. Gains effect was defined as the average thermal niche of species that were newly recorded in the resurvey but absent from the baseline survey minus the baseline T_{CWM}, while losses effect was calculated as the baseline T_{CWM} minus the mean thermal niche of species that disappeared between the baseline survey and resurvey. Gains effect describes the directional impact of novel species arrivals, and losses effect reflects the impact of species loss on thermal restructuring. Abundance shifts effect was quantified as ΔT_{CWM} between the two surveys using only the set of species identified in both baseline surveys and resurveys, weighted by their relative abundances in each survey, which captures compositional shifts among persisting species that contribute to warming or cooling, independent of species turnover. For each plot, we estimated gains and losses effects using the median of species-specific thermal niche distribution as the respective mean thermal difference relative to the baseline T_{CWM}. The abundance shift effect was estimated as the change in T_{CWM} over time based only on the subset of shared species in both surveys. The sum of the three effects yielded a total estimate (estimated ΔT_{CWM}), which was then compared to the observed ΔT_{CWM} to assess the explanatory power of mechanism. In addition, we estimated the relative contribution of each mechanism by dividing the absolute value of its effect by the sum of the absolute values of all three effects, and the contributions were then expressed as percentages to facilitate comparison among mechanisms. We identified the dominant mechanism for each plot as the one with largest percentage contribution. Results showed significant linear relationships between estimated and observed ΔT_{CWM} across ecosystems, with R^2 values ranging from 0.23 to 0.53 (Extended Data Fig. 4b), indicating that

the three mechanisms collectively provide a reasonable explanation for observed thermophilization patterns. Building on this, results further suggested that gains and losses were the dominant contributors to thermophilization of understory vegetation in forests, losses played the primary role in grasslands, while losses and abundance shifts of persisting species were the major contributor on alpine summits (Extended Data Fig. 4a). These results highlight that the relative importance of gains, losses, and abundance shifts in driving thermophilization is ecosystem-dependent, reflecting distinct community dynamics and responses to climate warming across ecosystems.

Despite the widespread use of the climatic debt metric by comparing ΔT_{clim} and ΔT_{plant}, it may neglect the variation in thermal niche space within a community, because one can get a climate debt yet background observed climate of the resurvey remains in the thermal niche space of all species in a community. Therefore, to test the robustness of the climatic debt results in our study, we further quantified the thermal suitability of background climate for plant communities, and also assessed the extent to which species in each community, at the plot level, were exposed to background climatic conditions beyond their thermal tolerance ranges. Specifically, for thermal niche suitability, we estimated the probability density of floristic temperature distribution (i.e., T_{plant}) at the observed climatic temperature (i.e., T_{clim}) for each plot and survey time. T_{plant} distribution were generated using the 1000 resampled values of species-specific thermal niches and abundance data, as described above. Then, for each value of the distribution, we computed a kernel density estimate (KDE) and extracted the probability density at the corresponding T_{clim} value using linear interpolation. The change in probability density between baseline survey and resurvey indicates whether the local climate has become more or less aligned with the

community's realized thermal niche, and a decline in density suggests an increasing mismatch between climate and community thermal preferences. Results showed significant and marginal declines in the probability density at T_{clim} from baseline survey to resurvey in forests and grasslands, respectively (Extended Data Fig. 5a), suggesting increasing climatic mismatch. However, no change in the probability density at T_{clim} was detected on alpine summits. Further, to estimate the proportion of thermally mismatched species, we derived each species' 2.5^{th} and 97.5^{th} percentiles of the thermal niche distribution. For each plot and survey time, we identified all recorded species and classified each as "thermally mismatched" if the background T_{clim} fell outside its thermal niche bounds (i.e., between the 2.5^{th} and 97.5^{th} percentiles of thermal niche distribution). We then calculated the proportion of mismatched species per plot as the number of mismatched species divided by the total number of species present, and estimated the change between resurvey and baseline survey. This metric thus captures the prevalence of species experiencing thermal stress relative to their historical niche distribution. We found that the proportion of mismatched species showed a significant increase in forests, but not in grasslands or on alpine summits (Extended Data Fig. 5b). These results suggest that thermal mismatch is progressing unevenly across ecosystems. In forests, the observed increase in mismatched species, together with declining probability density, indicates that climatic conditions are moving away from the realized thermal preferences of the plant community. In contrast, the lack of detectable change in grasslands and summits may reflect either reduced climatic displacement relative to forests or species assemblages with broader thermal affinities. Overall, these findings suggest that comparing difference in ΔT_{clim} and ΔT_{plant} may have overestimated climatic debts in grasslands and alpine summits, and refine our understanding of climate debt by highlighting both directional responses and ecosystem-specific characteristics in tracking

750 climate change.

751

752 Alpine summits are characterized by rugged topographic gradients that generate strong
753 microclimatic heterogeneity, which may have strong impacts on vegetation thermophilization.
754 To assess the potential impacts of alpine summit topography on thermophilization, we derived
755 terrain ruggedness index (TRI) and slope data from a 30-meter resolution digital elevation
756 model (DEM) using the *terrain* function from the *terra* R package, and extracted snow cover
757 data from CHELSA version 2.1 with a resolution of 30 arc-sec (~1 km)[73]. We found that neither
758 TRI nor slope showed significant relationships with thermophilization rates (Extended Data Fig.
759 3a), likely because in our database only summit-level coordinates were available, and metrics
760 such as TRI fail to capture the fine-scale microclimate that more strongly influence community
761 responses. However, we found that thermophilization rate was significantly lower in north-
762 facing slopes compared to south-facing slopes, and that snow cover change rate was lowest on
763 northern aspects (Extended Data Fig. 3b). These results indicate that microclimatic habitats,
764 generated by rugged topographic gradients and slope aspect, could be a key mechanism in
765 shaping thermophilization patterns on alpine summits. To further evaluate whether the use of
766 20 × 20 km temperature data would bias the estimation of thermophilization rates on alpine
767 summits, given that data at such a resolution may not adequately capture the fine-scale thermal
768 conditions experienced by alpine plants, we extracted the climatic data of monthly mean
769 temperature of the growing season from WorldClim v.2 as a raster file with 30 arc-sec resolution
770 (~1 × 1 km)[62], and re-estimated thermophilization rates on alpine summits using the same
771 method and compared with those estimated using 20 × 20 km resolution temperature data.
772 Results showed that the two sets of estimates were strongly correlated (Extended Data Fig. 8a),

and only a small difference was found between the thermophilization rates of the 95th percentile as estimated using Bayesian mixed-effects models (Extended Data Fig. 8b). Nevertheless, this difference will not affect the interpretation of the overall patterns of thermophilization on alpine summits, demonstrating a high degree of consistency between the estimation of thermophilization derived from fine and coarse resolution climate data, indicating that the use of the 20 × 20 km resolution data remains appropriate and our core conclusions are robust to the choice of climate data resolution.

To evaluate whether spatial autocorrelation might bias the ecosystem effects on thermophilization rates, we incorporated a spatial Gaussian Process (GP) term into our Bayesian mixed-effects models[74]:

thermophilization rate ~ ecosystem_type + plot_size + $T_{clim_baseline}$ + gp(longitude, latitude) + (1|site)

and then compared the posterior distributions of the fixed-effect estimates for ecosystem type between the spatial and non-spatial model specifications. Results showed a high degree of consistency, with substantial overlap in the 95% CIs (Extended Data Fig. 8c). This strong agreement between the models indicates that spatial autocorrelation did not influence the estimated ecosystem effects, likely because that the random intercept for "site" captured most of the large-scale spatial structure. Given the robustness of the estimates and for the sake of model parsimony, we therefore presented the results from the simpler, non-spatial models.

Sources of uncertainty

Although we document general patterns of vegetation thermophilization and climatic debts here, uncertainties remain reflecting inherent limitations in the data. First, declines and increases in species abundance may reflect sampling variation (e.g., shifts in plant locations or inexact placement of quasi-permanent plots) rather than actual community changes between baseline surveys and resurveys, and the inclusion of quasi-permanent plots may thus influence the overall patterns of vegetation response to warming. In our study, all the plots on alpine summits are permanent, while most plots are quasi-permanent in forests and grasslands. Regardless of their formal designation, all plots were relocated using high-precision GPS coordinates or clearly documented map references, ensuring accurate re-surveys across time. While metadata did not always distinguish between permanent and quasi-permanent plots, the relocation accuracy was closely comparable across plot types. Importantly, we restrict our inferences to averages across plots and at the community level rather than focusing on results from individual plots. Hence, small relocation errors only add some uncertainty to results rather than introducing any systematic bias in the magnitude or direction of effects at the community level (thermophilization). In addition, many plants move over time, meaning even exactly relocated permanent plots show shifts in composition and abundance. Our key conclusions are robust to these sources of noise as supported by a previous study using a subset of the forest plots in our dataset. This study showed that the impact of relocation errors is very limited when focusing on overall temporal changes in vegetation communities[75]. As such, the inclusion of both types of plots does not introduce systematic bias or influence the observed ecosystem-level patterns[75,76].

Second, although our study provides a unique opportunity to compare vegetation responses to

climate warming across ecosystems using harmonized plot-level resurveys and standardized climate metrics, we acknowledge that full methodological standardization was not possible. The underlying datasets were originally collected by different monitoring networks using varying survey protocols, plot sizes, and time intervals. These differences may introduce some uncertainty into cross-ecosystem comparisons. Nevertheless, by applying consistent analytical methods and filtering to include only plots with comparable abundance data, we minimized potential bias and ensured the robustness of our main conclusions.

Third, another source of uncertainty may stem from the variation in time intervals between the baseline survey and resurvey across plots (Extended Data Fig. 1a). Some plots span multiple decades and thus are more likely to capture pronounced climatic changes, whereas others have shorter intervals with potentially weaker climate signals. This temporal heterogeneity, which also differs somewhat among ecosystems, may influence the observed rates of thermophilization. Although such variation is inherent in resurvey-based studies and reflects logistical and historical constraints, it represents an important consideration when interpreting the strength and consistency of observed patterns.

At last, the distribution of our plots was skewed toward Northern and Central Europe, with comparatively fewer sites in Southern Europe (Fig. 1). While the dataset still covers a broad range of European climatic and ecological gradients and is thus suitable for continental-scale analysis, this spatial imbalance would still represent a source of uncertainty. Future research should aim to increase plot coverage in underrepresented Southern regions of Europe, to ensure more robust and spatially comprehensive assessments of thermophilization patterns.

50 Verheyen, K. *et al.* Combining biodiversity resurveys across regions to advance global change research. *BioScience* **67**, 73-83 (2017).

51 Gilliam, F. S. The Ecological Significance of the Herbaceous Layer in Temperate Forest Ecosystems. *BioScience* **57**, 845-858, doi:10.1641/B571007 %J BioScience (2007).

52 Hermy, M., Honnay, O., Firbank, L., Grashof-Bokdam, C. & Lawesson, J. E. An ecological comparison between ancient and other forest plant species of Europe, and the implications for forest conservation. *Biological Conservation* **91**, 9-22, doi:https://doi.org/10.1016/S0006-3207(99)00045-2 (1999).

53 Peterken, G. F. *Natural woodland: ecology and conservation in northern temperate regions*. (Cambridge University Press, 1996).

54 Peeters, A. *et al.* in *Grassland Science in Europe* 743-750 (European Grassland Federation, 2014).

55 Diekmann, M. *et al.* Patterns of long-term vegetation change vary between different types of semi-natural grasslands in Western and Central Europe. *Journal of Vegetation Science* **30**, 187-202 (2019).

56 Pauli, H. *et al. The GLORIA field manual: Standard multi-summit approach, supplementary methods and extra approaches*. (GLORIA-Coordination, Austrian Academy of Sciences & University of Natural, 2015).

57 Kapfer, J. *et al.* Resurveying historical vegetation data – opportunities and challenges. *Applied Vegetation Science* **20**, 164-171, doi:https://doi.org/10.1111/avsc.12269 (2017).

58 Staude, I. R. *et al.* Directional turnover towards larger-ranged plants over time and across habitats. *Ecology Letters* **25**, 466-482 (2022).

59 Lenoir, J. *et al.* Local temperatures inferred from plant communities suggest strong spatial buffering of climate warming across Northern Europe. *Global Change Biology* **19**, 1470-1481, doi:https://doi.org/10.1111/gcb.12129 (2013).

60 Pau, S. *et al.* Predicting phenology by integrating ecology, evolution and climate science. *Global Change Biology* **17**, 3633-3643, doi:https://doi.org/10.1111/j.1365-2486.2011.02515.x (2011).

61 Cheung, W. W. L., Watson, R. & Pauly, D. Signature of ocean warming in global fisheries catch. *Nature* **497**, 365-368, doi:10.1038/nature12156 (2013).

62 Fick, S. E. & Hijmans, R. J. WorldClim 2: new 1-km spatial resolution climate surfaces for global

land areas. *International Journal of Climatology* **37**, 4302-4315, doi:https://doi.org/10.1002/joc.5086 (2017).

63 Gaston, K. J. & Fuller, R. A. The sizes of species' geographic ranges. *Journal of Applied Ecology* **46**, 1-9, doi:https://doi.org/10.1111/j.1365-2664.2008.01596.x (2009).

64 Peterson, A. T. *et al. Ecological niches and geographic distributions*. Vol. 49 (Princeton University Press, 2011).

65 Staude, I. R. *et al.* Replacements of small- by large-ranged species scale up to diversity loss in Europe's temperate forest biome. *Nature Ecology & Evolution* **4**, 802-808, doi:10.1038/s41559-020-1176-8 (2020).

66 Rodríguez-Sánchez, F., De Frenne, P. & Hampe, A. Uncertainty in thermal tolerances and climatic debt. *Nature Climate Change* **2**, 636-637 (2012).

67 Bürkner, P.-C. brms: An R Package for Bayesian Multilevel Models Using Stan. *Journal of Statistical Software* **80**, 1 - 28, doi:10.18637/jss.v080.i01 (2017).

68 Dushoff, J., Kain, M. P. & Bolker, B. M. I can see clearly now: Reinterpreting statistical significance. *Methods in Ecology and Evolution* **10**, 756-759, doi:https://doi.org/10.1111/2041-210X.13159 (2019).

69 Mazalla, L. & Diekmann, M. Regression to the mean in vegetation science. *Journal of Vegetation Science* **33**, e13117, doi:https://doi.org/10.1111/jvs.13117 (2022).

70 McGill, B. J. Linking biodiversity patterns by autocorrelated random sampling. *American Journal of Botany* **98**, 481-502, doi:https://doi.org/10.3732/ajb.1000509 (2011).

71 MacKenzie, D. I. *et al. Occupancy estimation and modeling: inferring patterns and dynamics of species occurrence*. (Academic Press, 2017).

72 Talluto, L., Boulangeat, I., Vissault, S., Thuiller, W. & Gravel, D. Extinction debt and colonization credit delay range shifts of eastern North American trees. *Nature Ecology & Evolution* **1**, 0182, doi:10.1038/s41559-017-0182 (2017).

73 Karger, D. N. *et al.* Climatologies at high resolution for the earth's land surface areas. *Scientific Data* **4**, 170122, doi:10.1038/sdata.2017.122 (2017).

74 Banerjee, S., Carlin, B. P. & Gelfand, A. E. *Hierarchical modeling and analysis for spatial data*. (Chapman and Hall/CRC, 2003).

75 Verheyen, K. *et al.* Observer and relocation errors matter in resurveys of historical vegetation plots.

Journal of Vegetation Science **29**, 812-823, doi:https://doi.org/10.1111/jvs.12673 (2018).

76 Kopecký, M. & Macek, M. Vegetation resurvey is robust to plot location uncertainty. *Diversity and Distributions* **21**, 322-330, doi:https://doi.org/10.1111/ddi.12299 (2015).

77 Verheyen, K. *et al.* Driving factors behind the eutrophication signal in understorey plant communities of deciduous temperate forests. *Journal of Ecology* **100**, 352-365, doi:https://doi.org/10.1111/j.1365-2745.2011.01928.x (2012).

Acknowledgements

K.Y. would like to thank Prof. Dr. Yan Peng for her unwavering support in both personal and professional life, and Prof. Dr. Kun Guo for his kind help with data analyses. K.Y. acknowledges the supports from the National Natural Science Foundation of China (32271633 and 32011530426), the National Key Research and Development Program of China (2023YFF1305500), the Central-guided Local Science and Technology Development Fund Projects of Fujian Province (2023L3005), and the Alexander von Humboldt Research Fellowship for Experienced Researchers. P.D.F. and P. Vangansbeke acknowledge the supports by the European Research Council (ERC) under the Horizon 2020 research and innovation program (ERC Starting Grant FORMICA 757833 and ERC Consolidator Grant CanopyChange 101124948) and from the Research Foundation – Flanders (FWO) by funding the scientific research network FLEUR (W000322N, www.fleur.ugent.be). A.D.B. was supported by the Knut and Alice Wallenberg Foundation (WAF KAW 2019.0202). M.K. and M. Macek. were supported by the Czech Science Foundation (project GACR 23-06614S), R.H., M.C. and O.V. were supported by the Czech Science Foundation (project 21-11487S), and M.K., M. Macek., R.H., M.C. and O.V. were founded by the Czech Academy of Sciences long-term development project (RVO 67985939). A.B.-S. was supported by European Union: Agricultural Fund for

Rural Development (EAFRD), Conseil Départemental de La Réunion and the Centre de Coopération internationale en Recherche agronomique pour le Développement (CIRAD). T.-M.U. acknowledges the support from the Ministry of Research, Innovation and Digitization of Romania through the Core Project BioClimpact no. 7/30.12.2022, code 23020401. P.D.T. was founded by the GreenMount project PN-IV-P2-2.1-TE-2023-0726 from UEFISCDI Romania. F. Máliš was supported by project VEGA 1/0245/25. This study is an outcome of the sREplot working group supported by sDiv, the Synthesis Centre of the German Centre for Integrative Biodiversity Research (iDiv) Halle-Jena-Leipzig (DFG FZT 118).

Author contributions

K.Y. and P.D.F. conceived, designed, and supervised the project. P. Vangansbeke , I.H.M.-S., D.M.W., K.V., M.B.-R., L.B., I.R.S., A.D.B., R.H., C.A., E.B., T.B., A.B.-S., J.-L.B.-A., J. Bennie, I.B., V.B., J. Brunet, J. Bullock, H.V.C., M. Carbognani, M. Chudomelová, D.C.-K., P.D.T., G.N.D., G.D., J.D., M.D., T. Dirnböck, T. Durak, O.E., B.E., B.J.G., T.H., M.H., P.H., U.J., B.J., R.K., J.K., M.K, T.K., A.L., J.L., M. Macek, M. Malicki, F. Máliš, O.M., F. Mitchell, T.N., T.A.N., M.N., A.C.N., L.N., L.O., A.O., S.O., A.O.-A., J.d.O., H.P., G.P., P.P., R.P., M.P., C.R., K.R., C.R., F.H.S., W.S., J.Š., A.S.-S., T.S., K.Ś., B.T., J.-P.T., T.-M.U., T.V., M.V., P. Vergeer, O.V., L.V., P. Vittoz, M.W., S.W., P.D.F. are the members of the data related working groups and/or contribute to data. K.Y., P. Vangansbeke, F.W., S.Z. and P.D.F. performed the statistical analyses. K.Y. developed the manuscript, with contributions and editing from all co-authors.

Competing interests

The authors declare no competing interests.

Additional information

Supplementary Information The online version contains supplementary material available at

Correspondence and requests for materials should be addressed to Kai Yue.

Peer review information *Nature* thanks and the other, anonymous, reviewer(s) for their contribution to the peer review of this work.

Reprints and permissions information is available at http://www.nature.com/reprints.

Data availability

Raw data used in this study are available at figshare (https://doi.org/10.6084/m9.figshare.28368743.v5). Other publicly available datasets used in the study include climate data from CRU TS version 4.07 (https://crudata.uea.ac.uk/cru/data/hrg/cru_ts_4.07) and WorldClim v.2 (https://rmets.onlinelibrary.wiley.com/doi/10.1002/joc.5086), topography data from the R package *elevatr* (https://cran.r-project.org/web/packages/elevatr), species occurrence records from GBIF (https://doi.org/10.15468/dl.hffjcf), and snow cover data from CHELSA version 2.1 (https://chelsa-climate.org/downloads).

Code availability

R code used in this study is available at figshare (https://doi.org/10.6084/m9.figshare.28368743.v5).

Extended Data Legends

Extended Data Fig. 1 | Frequency distributions of data for survey plots, climate, and plant species. a, Frequency distribution of plot at baseline and resurvey years in forest, grasslands, and alpine summits. **b,** Frequency distribution of growing season (April to September) mean temperature (T_{mean}) change rate across the duration of plant surveys in forests, grassland, and alpine summits. The rate of T_{mean} change for each plot was calculated as the difference between the average mean temperature during the 5 years preceding the baseline survey and the resurvey, divided by the time interval between the two surveys. The medians of the growing season T_{mean} change rate across forests, grasslands, and alpine summits were 0.31, 0.22, and 0.31 °C decade^{-1}, respectively. **c,** Frequency distribution of the number of grid cells representing species range sizes quantified by area of occupancy (AOO). Across the species pool in our study, 36.4% of the species have AOO < 1000, among which 77.5% of the species have AOO < 500. The green and blue dashed line indicate an AOO of 500 and 1000, respectively.

Extended Data Fig. 2 | Vegetation thermophilization rate and climatic debts (°C decade^{-1}) in forests, grasslands, and alpine summits estimated using different datasets. a, Vegetation thermophilization rate and climatic debt quantified as the loss of cold-adapted species (5th percentile shift), overall (median shift), and gain of warmth-demanding species (95th percentile shift) using plant presence/absence data excluding rare species. Circles represent means (n = 4372, 1209, and 457 plots for forests, grasslands, and alpine summits, respectively) with 80% (thick line) and 95% (thin line) credible intervals and posterior distributions obtained from Bayesian mixed-effects models. These results are similar with those estimated using plant abundance data excluding rare species in Fig. 2. **b,** Vegetation thermophilization rate and climatic debt quantified as the decline/loss of cold-adapted species (5th percentile shift), overall (median shift), and increase/gain of warmth-demanding species (95th percentile shift) using

plant abundance and presence/absence data including rare species. Circles represent means (n = 4372, 1209, and 486 plots for forests, grasslands, and alpine summits, respectively) with 80% (thick line) and 95% (thin line) credible intervals and posterior distributions obtained from Bayesian mixed-effects models. The overall patterns for thermophilization rate and climatic debt are in line with those estimated using plant data excluding rare species.

Extended Data Fig. 3 | Impacts of topography, snow cover and slope aspect on vegetation thermophilization rates on alpine summits. a, Relationships between thermophilization rates and terrain ruggedness index (TRI) and slope. Each point represents a plot (n = 457). Thermophilization rates were calculated using the median of the floristic temperature distributions that were estimated with vegetation abundance data excluding rare species. TRI and slope were derived from a 30-meter resolution digital elevation model (DEM) using the *terrain* function from the *terra* R package. **b,** Impacts of snow cover days and slope aspect on vegetation thermophilization rate. Thermophilization rates were estimated using vegetation abundance data excluding rare species, and data for snow cover were extracted from CHELSA version 2.1 (30 arc-sec resolution, ~1 km). Box plots show the median (centre line), the 25th and 75th percentiles (bounds of box), and the minimum and maximum values (whiskers). Each point represents a plot (n = 457), and a slight jitter was applied to the points to better visualize overlap, where applicable. Snow cover change rate was calculated as the difference in mean snow cover days between the five years preceding the baseline survey and the five years preceding the resurvey, divided by the time span (in decades) between the baseline and resurvey surveys. Shaded bands around fitted lines indicate 95% confidence intervals from linear mixed-effects models with "site" as a random effect. Different lowercase letters denote significant differences among slope aspects, based on linear mixed-effects models followed by Tukey's post-hoc tests (two-sided, adjusted for multiple comparisons at $p < 0.05$).

Extended Data Fig. 4 | Thermophilization explained by the mechanisms of species gains, losses, or abundance shifts in different ecosystems. a, Proportions of plots in which thermophilization was primarily driven by mechanisms of species gains, losses, or abundance

shifts. The dominant mechanism was identified for each plot as the one contributing the most (in absolute terms) to the observed shift in community thermal affinity. These results indicate that thermophilization was mainly driven by mechanisms of gains in grasslands, gains and losses in forests, and losses and abundance shifts on alpine summits. **b,** Relationship between observed *vs.* estimated community-weighted mean temperature (ΔT_{CWM}) for different ecosystem types without or with rare species. The sum of gains, losses, and abundance shifts of persisting species was used to estimate ΔT_{CWM} per plot and compared with the observed ΔT_{CWM}. Each point represents a plot (n = 4372, 1209, and 457 for forests, grasslands, and alpine summits, respectively), coloured by ecosystem type. Solid lines represent linear regression per ecosystem with 95% confidence intervals, and the dashed line denotes the 1:1 relationship. The significant linear relationships between estimated and observed ΔT_{CWM} indicate that the three mechanisms collectively provide a reasonable explanation for observed thermophilization patterns.

Extended Data Fig. 5 | Changes in the probability density of species thermal suitability and the proportion of thermally mismatched species in different ecosystems. a, Changes in the probability density of thermal suitability under local climate (T_{clim}) inferred from plot-level floristic temperature (T_{plant}) distributions. Boxplots showing changes in probability density of T_{plant} between baseline survey and resurvey (Δ = resurvey – baseline survey), with the centre line indicating the median, the box representing the 25th and 75th percentiles, and the whiskers showing the minimum and maximum values. These results show that the probability density at T_{clim} significantly and marginally decreased from baseline to resurvey in forest and grassland ecosystems, respectively, suggesting increasing climatic mismatch. **b,** Changes in the proportion of thermally mismatched species (Δ = resurvey – baseline survey). Mismatch is

defined as background macroclimate falling outside of the 2.5–97.5% range of a species' thermal distribution. These results suggest that the proportion of mismatched species significantly increased in forests, but not in grasslands or on alpine summits. In both figures, each point represents a plot (n = 4372, 1209, and 457 for forests, grasslands, and alpine summits, respectively), and the black circles with error bars indicate estimated means with 95% confidence intervals estimated using linear mixed-effects models with "site" as a random-effects factor, and the p values indicate whether change differs significantly from zero (linear mixed-effects models; two-sided).

Extended Data Fig. 6 | Quantile-quantile (QQ) plots of vegetation thermophilization rates and climatic debts (° C decade^{-1}). Each plot (n = 6038 and 6067 for estimations excluding and including rare species, respectively) compares the sample quantiles of the observed data with the theoretical quantiles of a normal distribution. The degree of alignment with the 1:1 reference line indicates how well each variable approximates normality, informing the suitability of linear modelling assumptions. GS05, GSMedian, and GS95 indicate the 5th, median, and 95th percentiles of the floristic temperature distribution estimated using mean growing season temperature, respectively, and ab and pa indicate the abundance and presence/absence vegetation data, respectively. These plots show an approximately linear relationship between theoretical and observed quantiles, indicating the deviations from normality were minimal and not severe enough to invalidate the Gaussian assumption.

Extended Data Fig. 7 | Climate warming patterns and vegetation thermophilization rate/climatic debt. a, Relationship between baseline temperature and temperature change rate

of the growing season across ecosystems and the associated residual plot. Each point represents a plot (n = 6038), with the red line indicating the linear regression fit and the shaded red area showing the 95% confidence interval. These visual and statistical diagnostics suggest that a linear baseline temperature term provides a reasonable adjustment in the estimation of thermophilization rate and climatic debt, with no strong evidence that a more complex or non-linear formulation is necessary in our analysis. **b,** Vegetation thermophilization rates and climatic debts (°C decade^{-1}) in different ecosystems as estimated using the 20% and 80% percentiles of the floristic temperature distribution. Thermophilization rate and climatic data were estimated using vegetation abundance data excluding rare species. Circles represent means (n = 4372, 1209, and 457 plots for forests, grasslands, and alpine summits, respectively) with 80% (thick line) and 95% (thin line) credible intervals and posterior distributions obtained from Bayesian mixed-effects models.

Extended Data Fig. 8 | Impacts of climate data resolution and spatial autocorrelation on vegetation thermophilization. a, Relationship between thermophilization rates estimated using fine (30 arc-sec, ~1 × 1 km) and coarse (10 arc-min, ~20 × 20 km) resolution climate data. Each point represents a plot (n = 457). The dashed lines represent the 1:1 relationship, while the solid black lines indicate the fitted linear regression with 95% confidence interval (gray shading). **b,** Overall thermophilziation rates estimated from Bayesian mixed-effects models using fine and coarse resolution climate data. Circles represent means (n = 457 plots) with 80% (thick line) and 95% (thin line) credible intervals and posterior distributions obtained from Bayesian mixed-effects models. Thermophilization rates were quantified as the declines of cold-adapted species (5th percentile shift), overall (median), and increases of warmth-demanding species (95th percentile shift) using vegetation abundance data excluding rare species. **c,** Comparison of estimated thermophilization rates (° C decade^{-1}) with and without accounting for spatial autocorrelation using a Gaussian Process (GP). Circles represent means

(*n* = 4372, 1209, and 457 plots for forests, grasslands, and alpine summits, respectively) with 80% (thick line) and 95% (thin line) credible intervals and posterior distributions obtained from Bayesian mixed-effects models. Thermophilization rates were quantified as the declines of cold-adapted species (5^{th} percentile shift), overall (median), and increases of warmth-demanding species (95^{th} percentile shift) using vegetation abundance data excluding rare species. The overlapping 95% CIs across models suggests that spatial autocorrelation does not confound the observed ecosystem differences in thermophilization, and that the ecosystem effects are robust to spatial structure.

Extended Data Table 1 | Detailed information on the databases of forests, grasslands, and alpine summits used in this study.

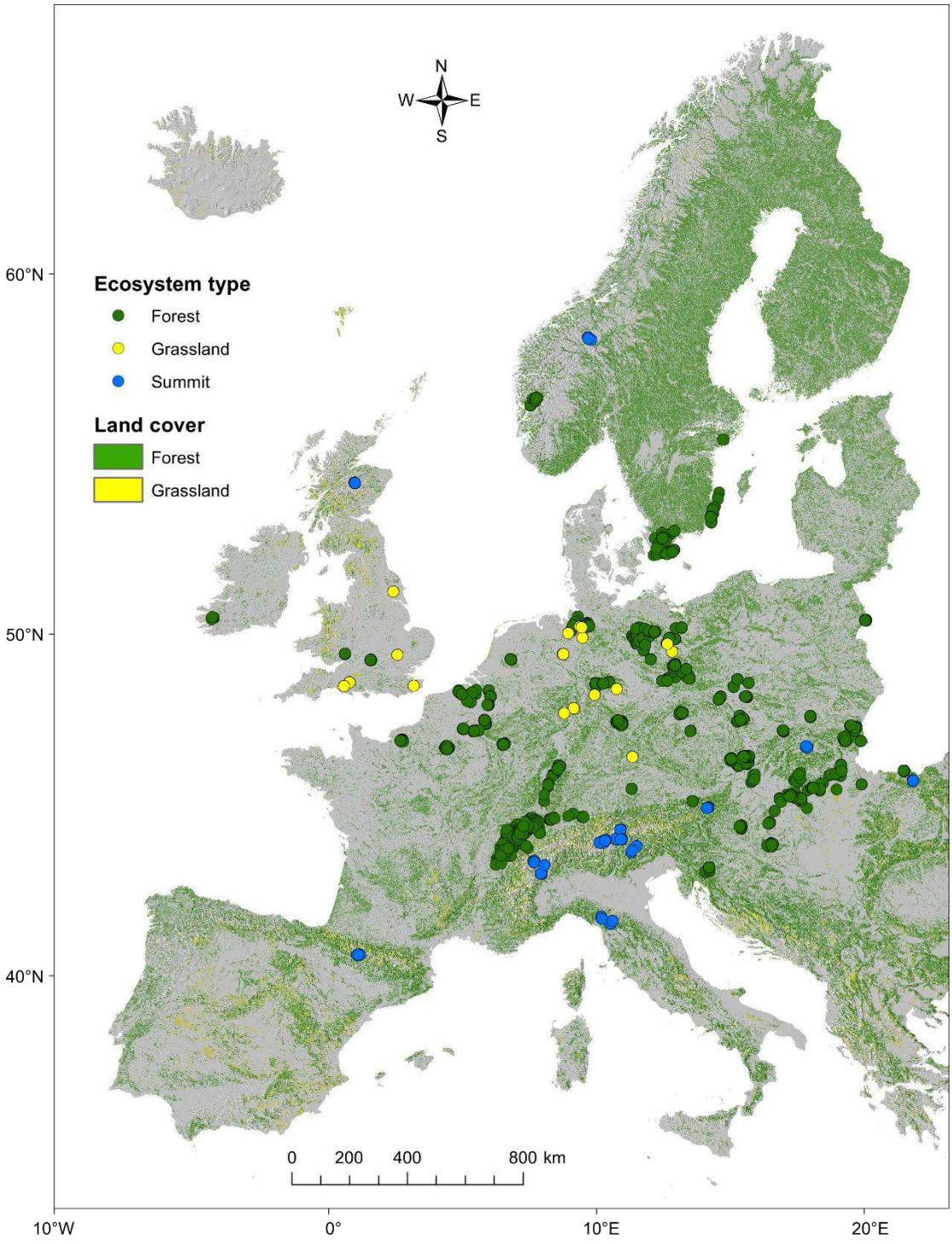

N
W
E
S
Ecosystem type
Forest
Grassland
Summit
Land cover
Forest
Grassland
60°N
50°N
40°N
0
200
400
800 km
10°W
0°
10°E
20°E

Figure 1

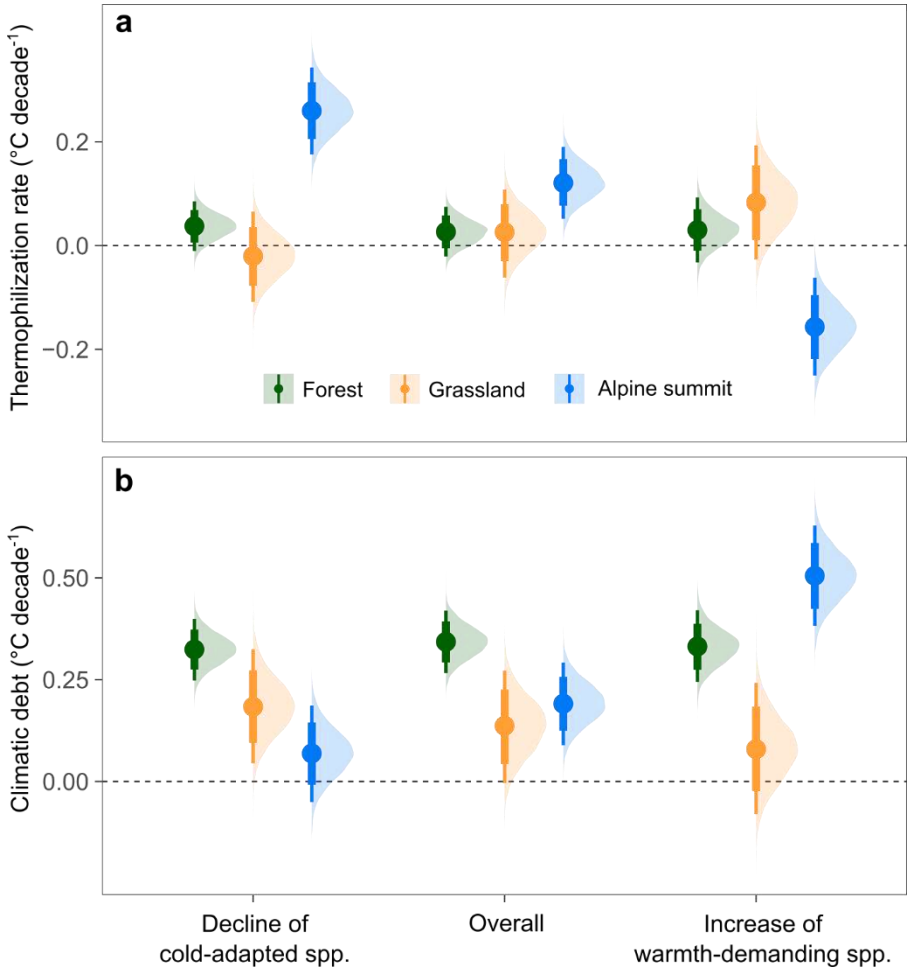

a
b
Thermophilization rate (°C decade-1)
Climatic debt (°C decade-1)
0.2
0.0
−0.2
0.50
0.25
0.00
Forest
Grassland
Alpine summit
Decline of cold-adapted spp.
Overall
Increase of warmth-demanding spp.

Figure 2

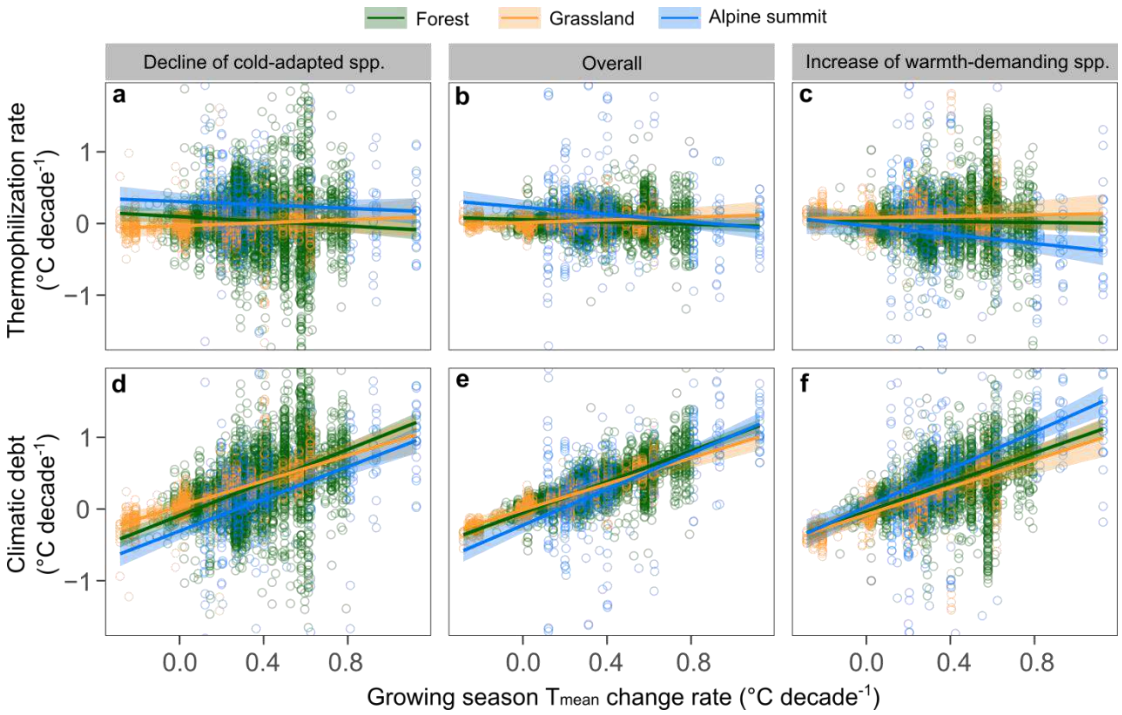
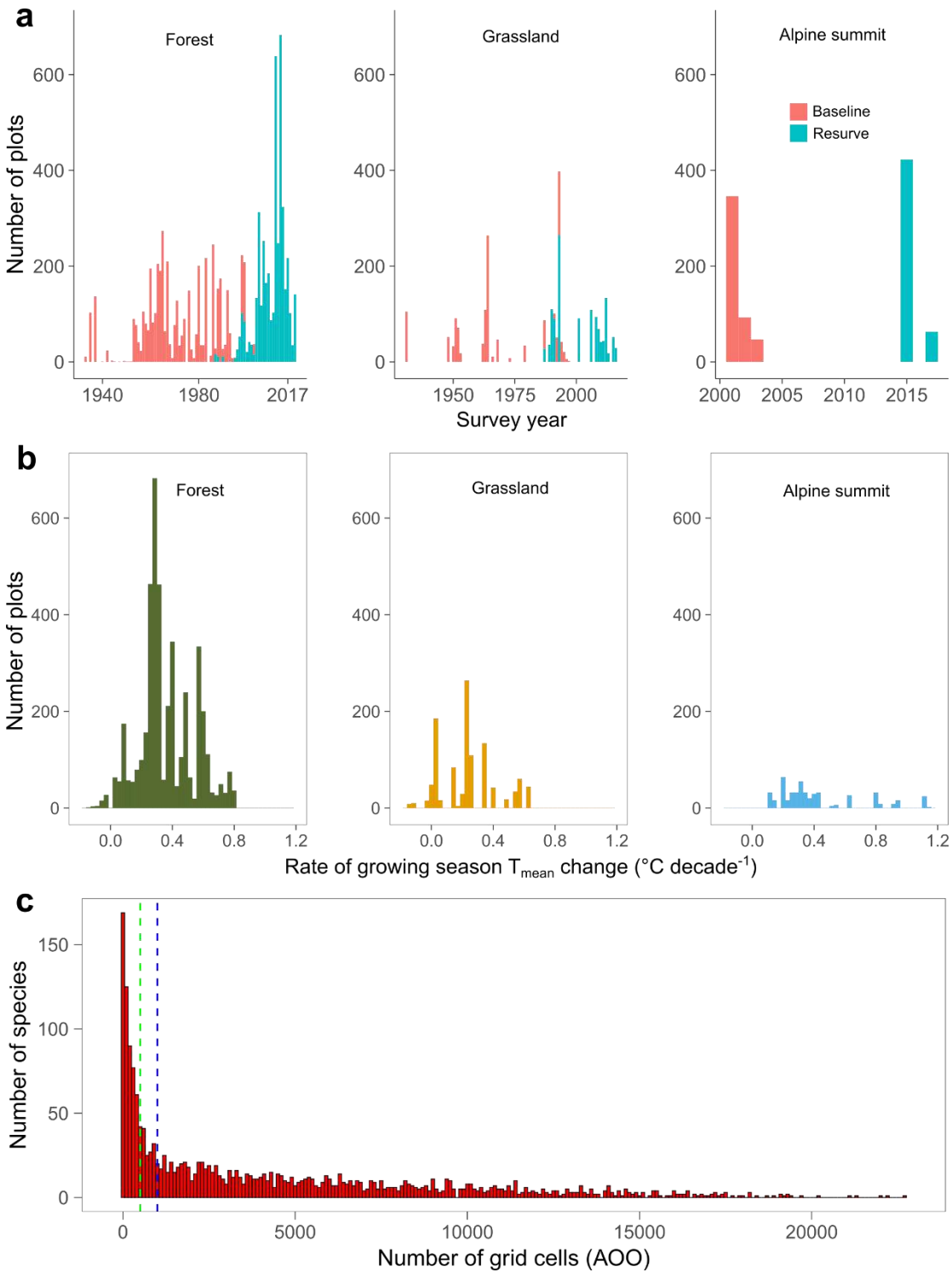
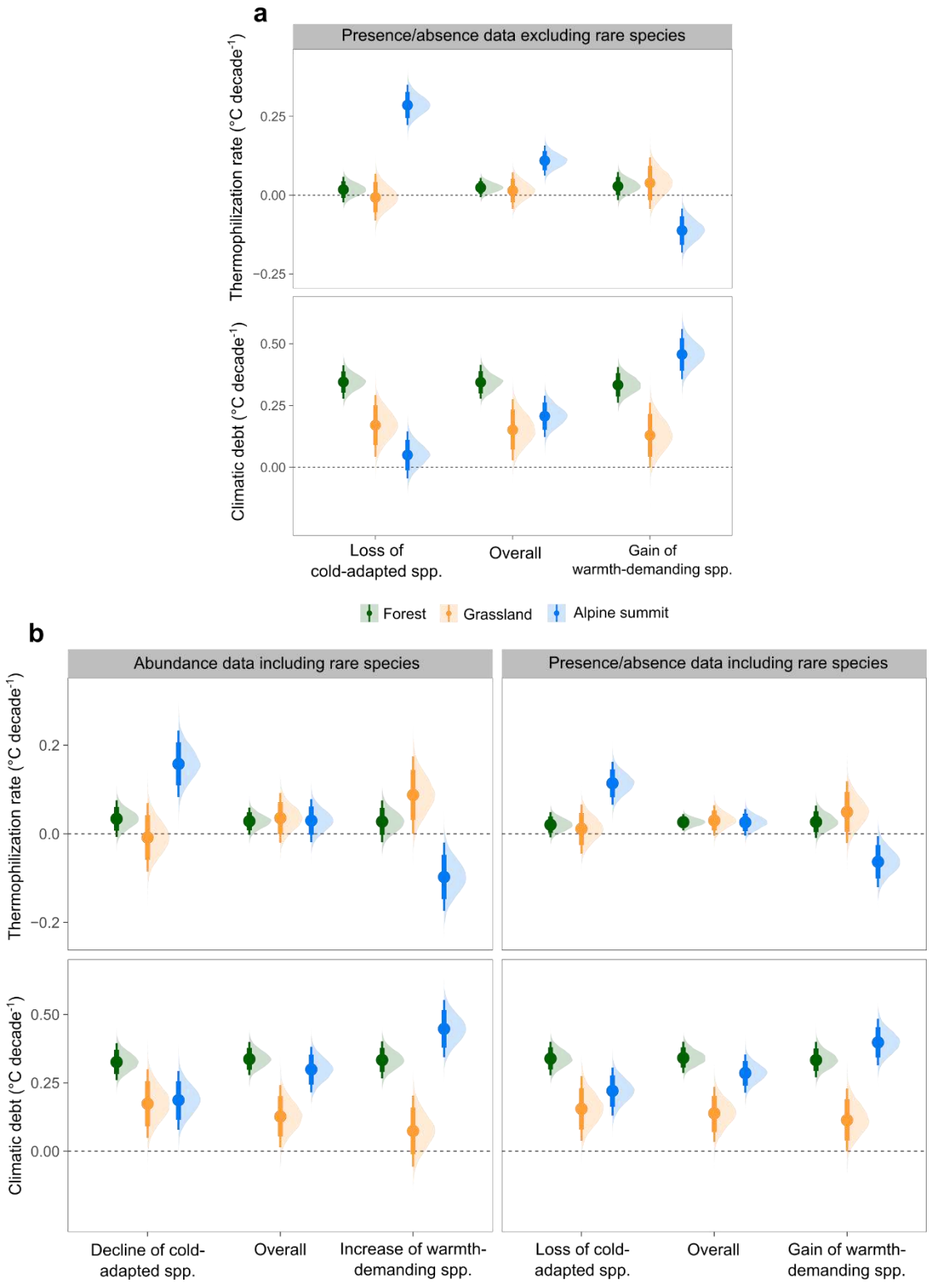

Forest
Grassland
Alpine summit
Decline of cold-adapted spp.
Overall
Increase of warmth-demanding spp.
a
b
c
d
e
f
Thermophilization rate (°C decade-1)
Climatic debt (°C decade-1)
1
0
−1
0.0
0.4
0.8
Growing season Tmean change rate (°C decade-1)

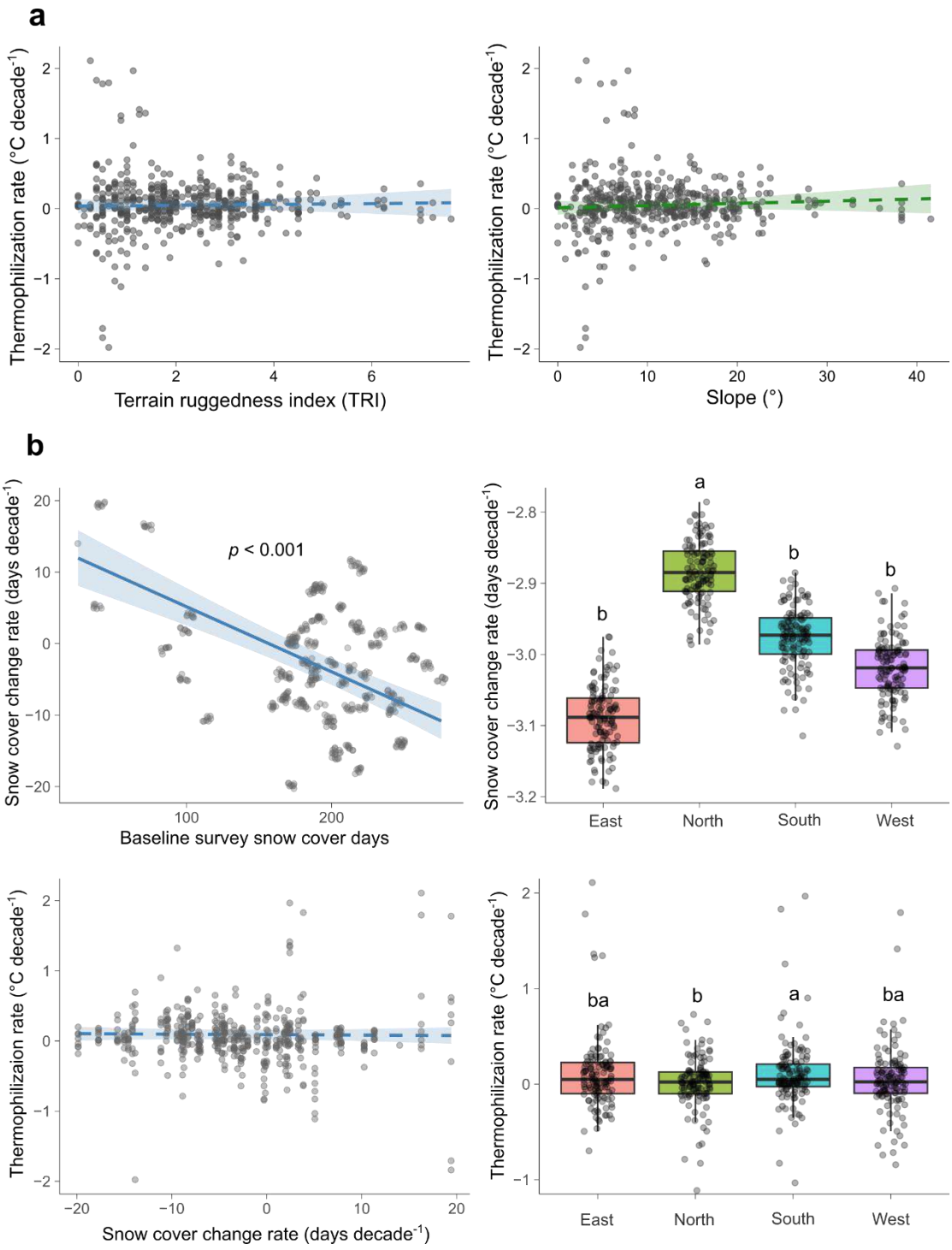
Figure 3



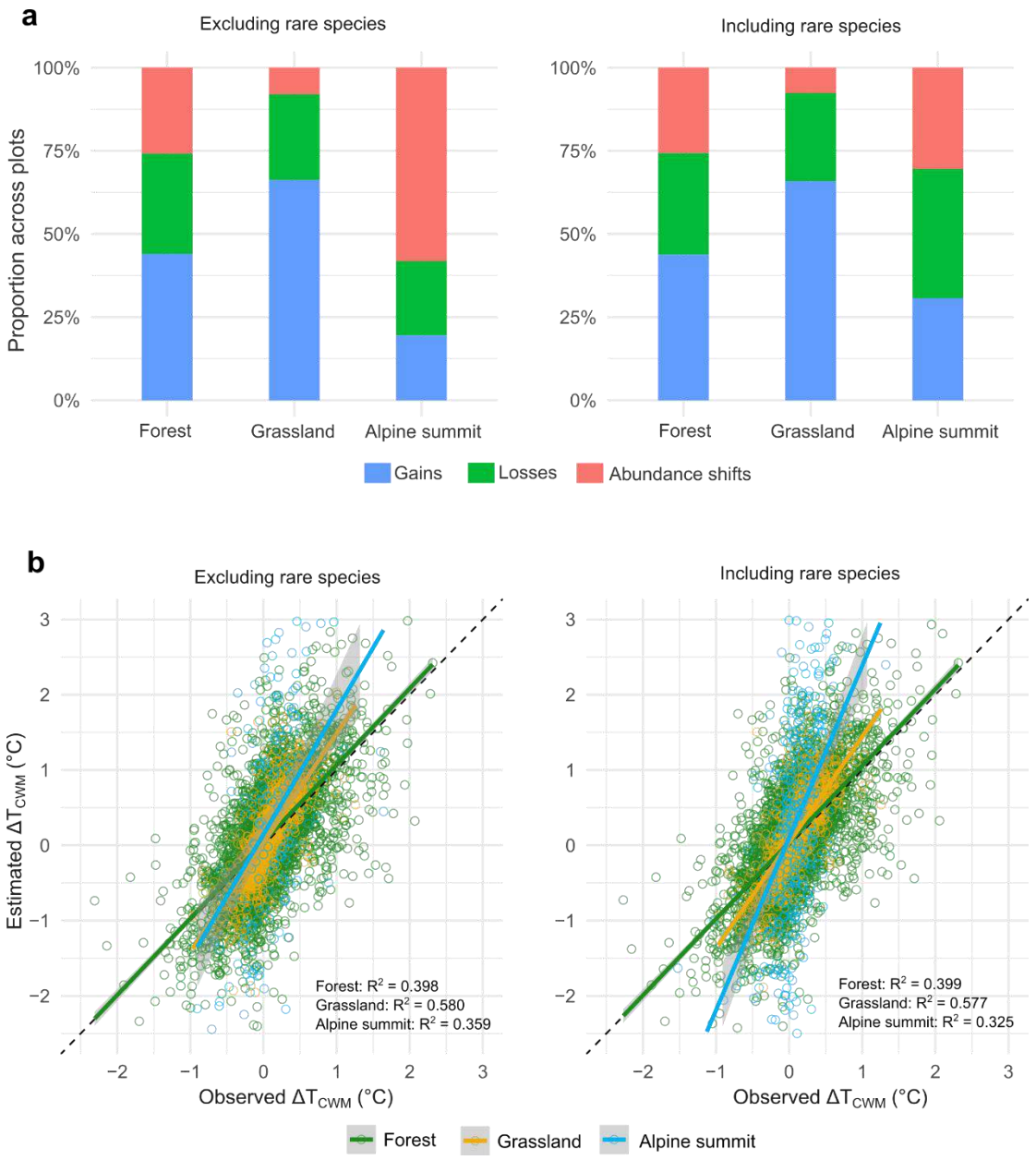
Extended Data Figure 1



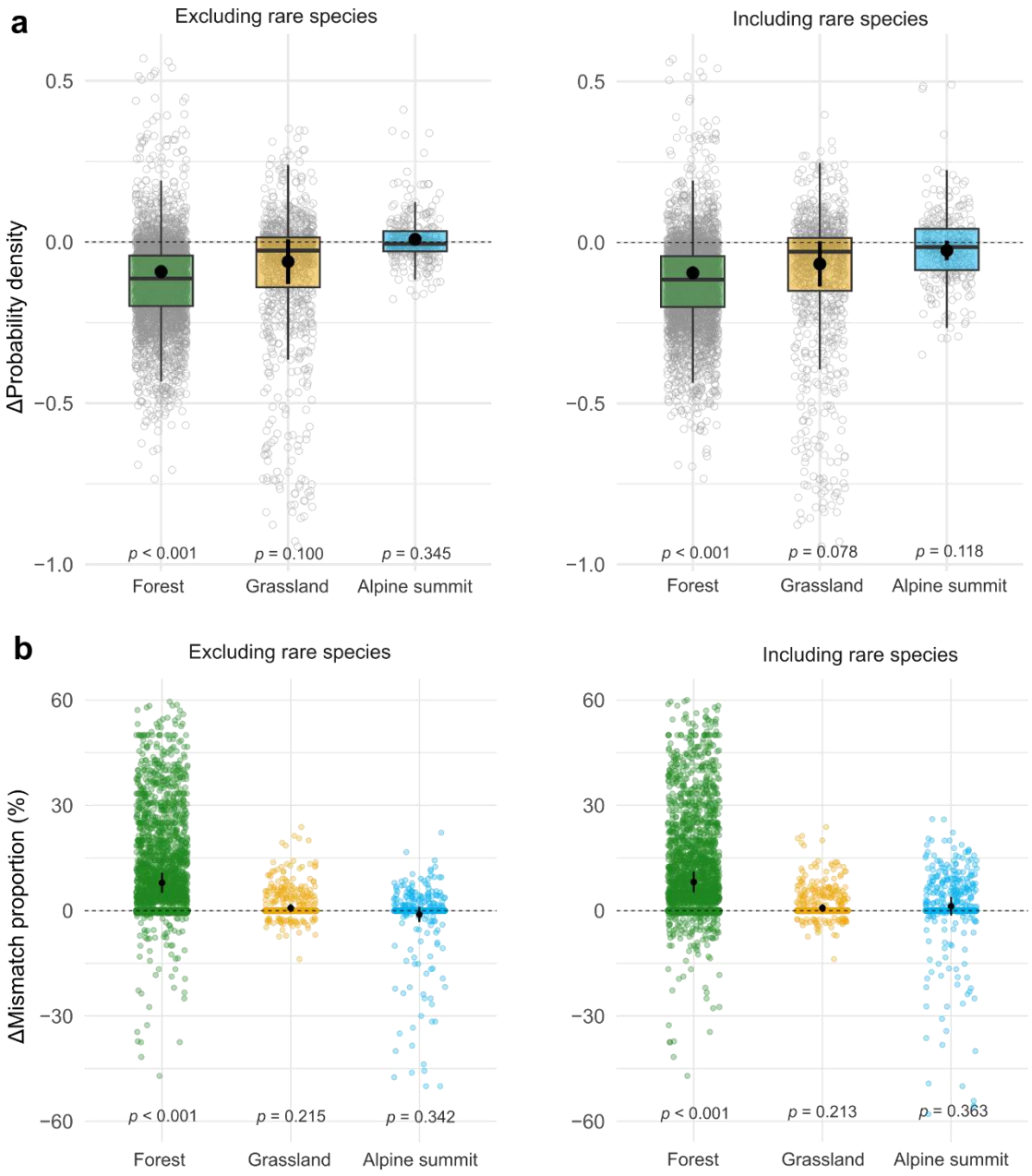
Extended Data Figure 2



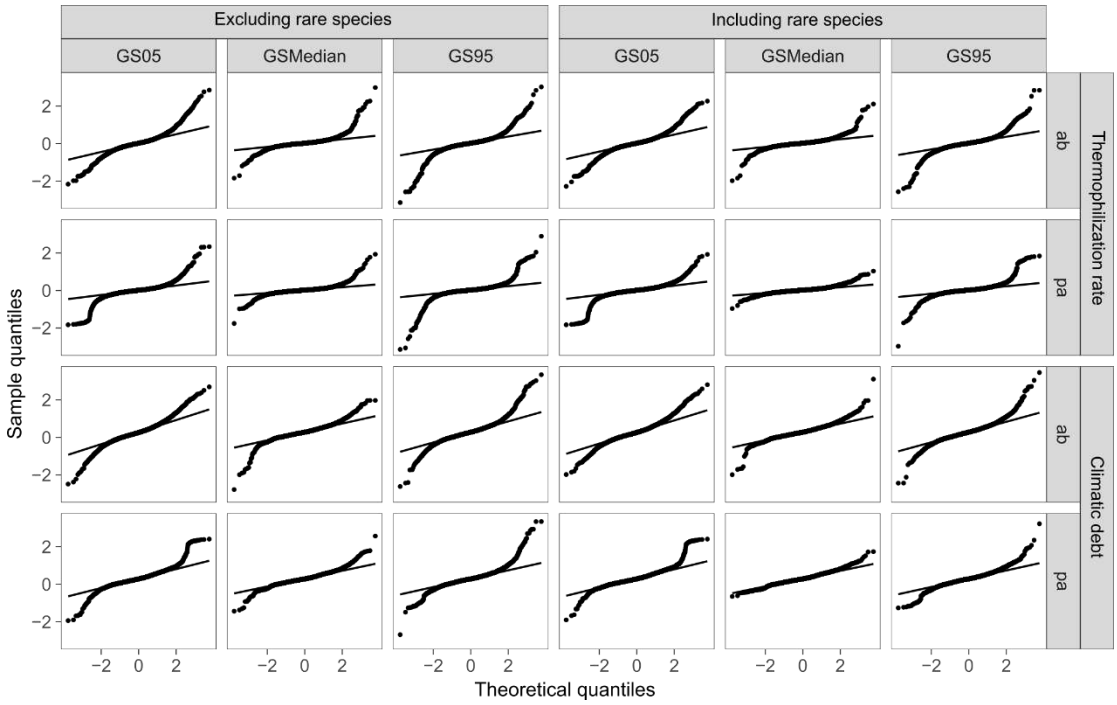
Extended Data Figure 3



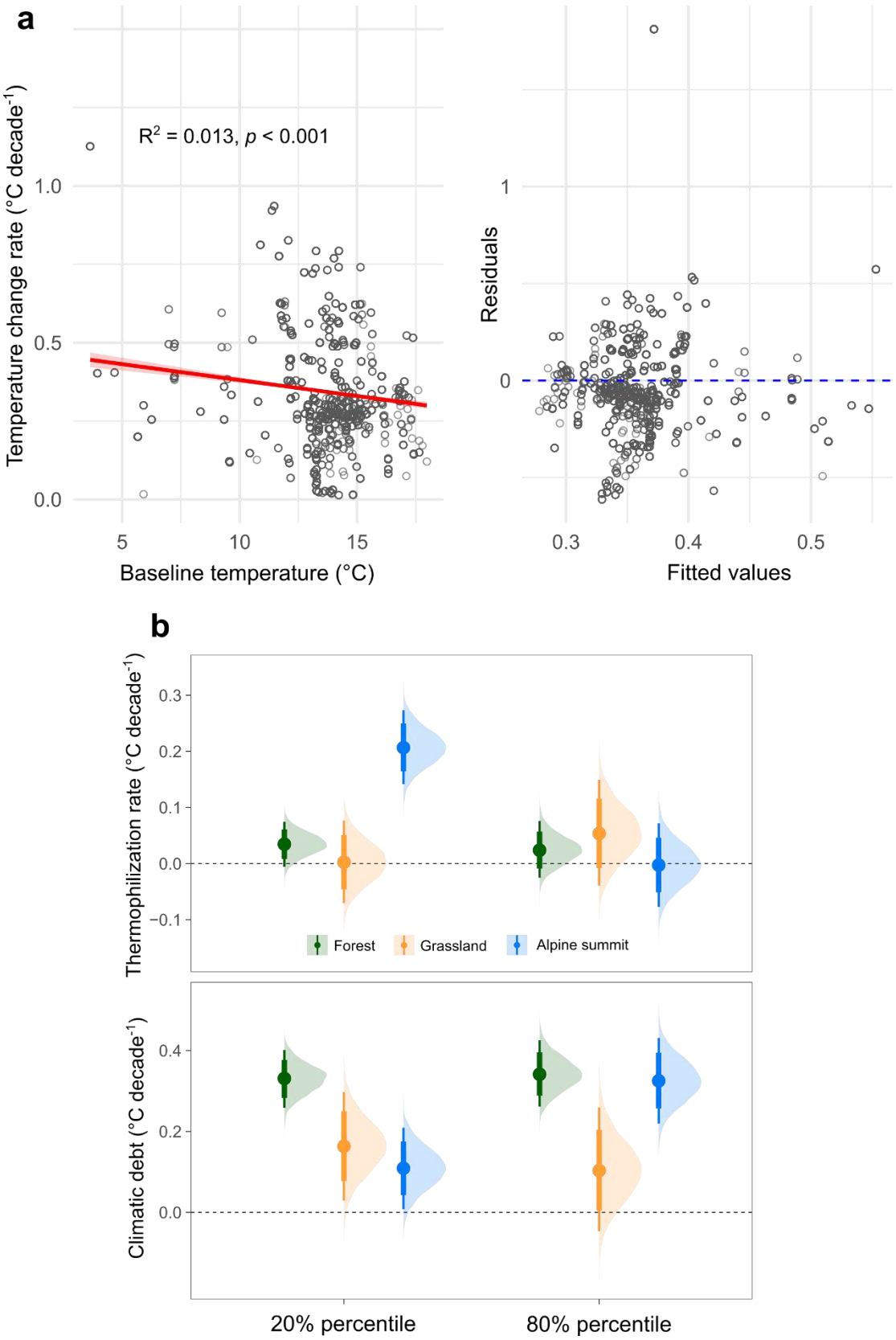
Extended Data Figure 4



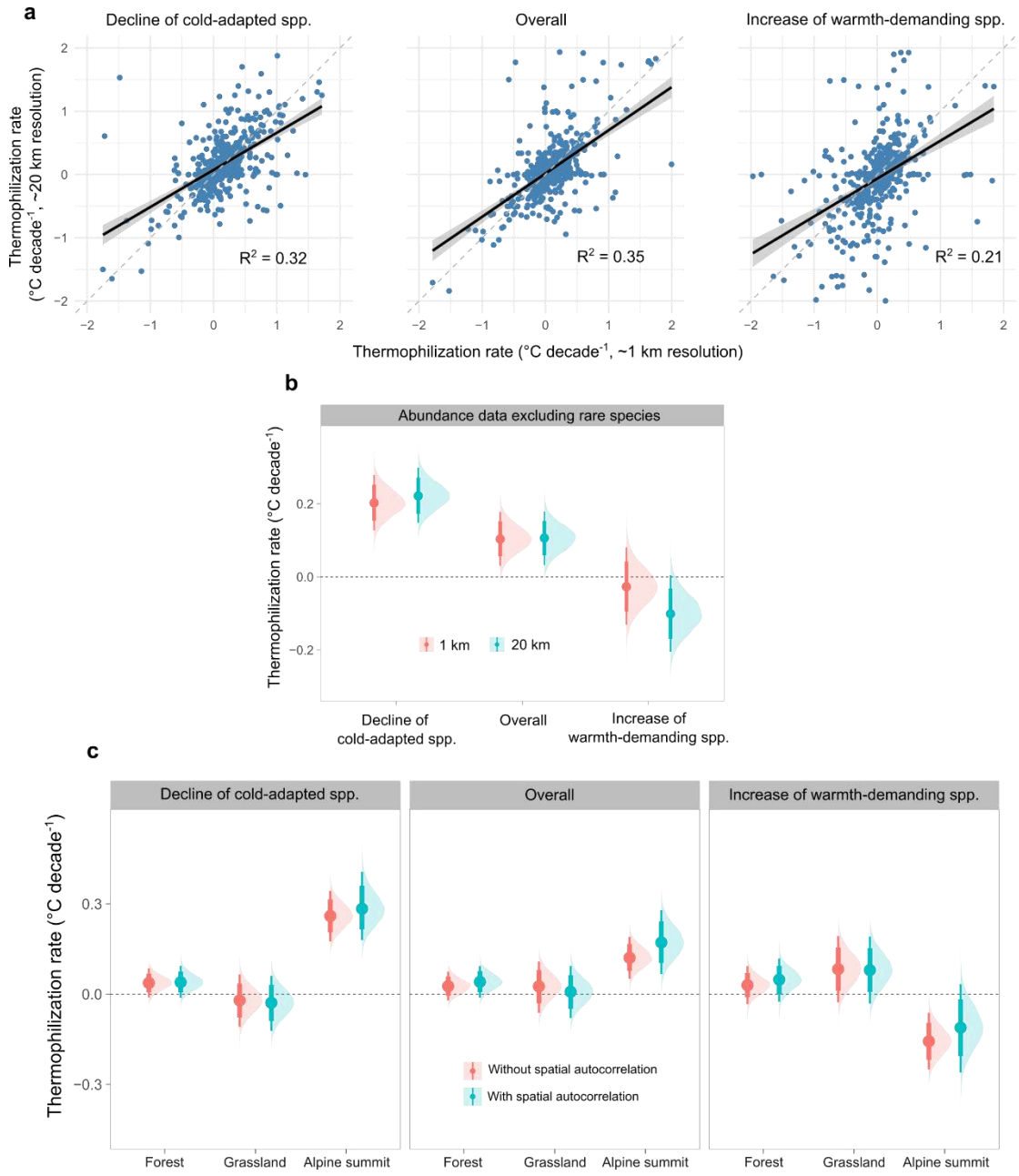
Extended Data Figure 5



Extended Data Figure 6



Extended Data Figure 7



Extended Data Figure 8

Ecosystem	Database	Number of plots	Number of sites	Earliest year of baseline survey	Latest year of resurvey	Range of intercensal time span (year)	Website	Key Reference
Forest	forestREplot	4372	76	1933	2020	12–78	forestreplot.ugent.be	Verheyen et al., 2012[77]
Grassland	GRACE	1209	22	1931	2016	16–78		Diekmann et al., 2019[55]
Alpine summit	GLORIA	486	64	2001	2017	12–15	gloria.ac.at	Pauli et al., 2015[56]

Extended Data Table 1